NASA Technical Memorandum 81948

NASA-TM-81948 19810011557

COMMENTS ON SETTLING CHAMBER DESIGN FOR QUIET, BLOWDOWN WIND TUNNELS

I. E. Beckwith

March 1981

National Aeronautics and Space Administration

Langley Research Center
Hampton, Virginia 23665

COMMENTS ON SETTLING CHAMBER DESIGN FOR QUIET, BLOWDOWN WIND TUNNELS

Ivan E. Beckwith
Langley Research Center

SUMMARY

The scheduled transfer of an existing continuous circuit supersonic wind tunnel to NASA Langley and its operation there as a blowdown tunnel has stimulated this review of flow disturbance requirements in the supply section and of recent methods developed to reduce the high level, broadband acoustic disturbances known to be present in typical blowdown tunnels. The indications are that the total turbulence levels, which include both the acoustic and vorticity modes, should be reduced to 1 percent or less in the settling chamber.

Based on recent data and the present analysis of two different blowdown facilities at Langley, methods to achieve these low levels of acoustic and vorticity disturbances are recommended. Included are pertinent design details of the damping screens and honeycomb and also the recommended minimum pressure drop across the porous components which will provide the required two orders of magnitude attenuation of the acoustic noise levels.

A suggestion for the support structure of these high pressure drop porous components is offered with the hope that detailed stress calculations and scale model tests will show whether this is a feasible approach to this most difficult problem.

INTRODUCTION

The scheduled transfer of the Jet Propulsion Laboratory (JPL) 20-Inch Supersonic Wind Tunnel to NASA Langley and its operation there as a blowdown wind tunnel requires a careful appraisal of the impact of the proposed supply piping system and new settling chamber design on flow quality. An important objective for the new installation is to achieve flow quality as good or better than experienced at JPL over the entire modified operating range which will be up to a stagnation pressure of 900 kPa (130 psia) and 130 kg/sec (280 lb/sec) mass flow rate. These conditions are more than twice the corresponding maximum levels used during its operation as a continuous, closed-circuit wind tunnel at JPL.

The Preliminary Engineering Report (PER), which was prepared for NASA by Sverdrup/ARO and provides a detailed engineering analysis of the transfer of the JPL tunnel, has clearly recognized these increased pressure and flow rates as potential problems that could cause serious degradation in flow quality. The term "flow quality" will herein be restricted to the acoustic noise and vorticity fluctuation levels in the test section flow. These two flow disturbance modes are often lumped together as "turbulence," and this combined meaning will be used throughout this report. The mean flow quality is determined primarily by the nozzle coordinates which will be assumed the same as before the move to Langley.

The purpose of the PER was not to provide the final design of the modified tunnel but only to identify all components to be replaced or modified and provide sufficient analysis to establish credibility of the approach. These requirements have been met by the PER which proposed a special "quiet" value and a new settling chamber. An 8.4 m (27.7 ft.) long entrance diffuser to the settling chamber would have four "filling" screens (to prevent separation) and an acoustic suppression chamber. The main chamber would be 2.44 m (8 ft.) in diameter by 6.5 m (21.4 ft.) long and would have a honeycomb and four turbulence screens. This approach would probably provide reasonably low vorticity disturbance levels at the new settling chamber exit but the acoustic noise levels there would depend on the noise characteristics (levels and spectrum) at the quiet valve inlet, the noise suppression and generation characteristics of the quiet valve itself, and the downstream acoustic treatment in the chamber. At this time most of these acoustic properties are not yet accurately known or specifiable since the design of the new high mass flow piping system and pressure reducing valves from the 2.9 x 10 kPa (4200 psi) air storage tanks is not yet finalized. The acoustic and vorticity disturbance characteristics of the exit flow from the quiet valve and even the availability of the valve are also unknown as of this writing.

Therefore, the main purpose of this note is to provide some aerodynamic design specifications for proven acoustic baffles and vorticity disturbance control components in the new settling chamber based on several years experience in developing and testing quiet, blowdown, supersonic tunnels at Langley (refs. 1-4) in the same facilities complex where the modified JPL tunnel will be located. Two different piping systems have been used in these tests and data have been obtained with control valves in both the choked and wide-open (usually unchoked) settings. The large amount of detailed data obtained in two different settling chambers during the quiet tunnel research program at Langley and the analysis provided in this report will show clearly for the first time that the high noise levels typical of control valves and piping systems for blowdown wind tunnels can be attenuated to the required low levels with relatively inexpensive components. Since the final design of the modified JPL tunnel is scheduled to start early in 1981, it is also appropriate to point out some potentially costly defects in the approach proposed in the PER to the turbulence control problems.

Use of trade names or names of manufacturers in this report does not constitute an official endorsement of such products or manufacturers, either expressed or implied, by the National Aeronautics and Space Administration.

SYMBOLS

A	cross-sectional, one-dimensional flow area
c	speed of sound
D	settling chamber diameter
d	screen wire diameter

F	turbulence reduction factor across multiple screens or essentially the ratio of $\tilde{u}/\bar{u}$ with screens to $\tilde{u}/\bar{u}$ without screens at the same x location usually taken at the asymptotic decay distance downstream of last screen
f	frequency
K	pressure drop coefficient across settling chamber components, $\Delta p/q_{sc}$
L	settling chamber length
ℓ	streamwise length of settling chamber components
M	Mach number
m	mesh size of settling chamber flow treatment component = reciprocal of mesh number per unit length for square mesh screens
$\dot{m}$	mass flow rate per unit area, ρu
n	number of multiple screens in series
p	pressure
q	dynamic pressure, $(1/2)\bar{\rho}\bar{u}^2$
R	unit Reynolds number
$\bar{R}$	ideal gas constant
r	radius
T	absolute temperature
u	velocity in x direction
x	axial distance
β	porosity of settling chamber flow treatment component = $1 - \sigma = \frac{\text{open area}}{\text{total area}}$
Δ	used as prefix to denote increment in a quantity
γ	ratio of specific heats
σ	solidity of settling chamber flow treatment component $= \frac{\text{solid area}}{\text{total area}}$
ρ	density

Subscripts

a	acoustic contribution
d	Reynolds number based on d
m	Reynolds number based on m
o	stagnation conditions in settling chamber downstream of all flow conditioner components
sc	flow conditions in settling chamber downstream of all flow conditioner components
v	vortical contribution
w	wall
∞	test section free stream
*	sonic flow

Superscripts

~	rms of fluctuating quantity
-	mean flow quantity

GENERAL REQUIREMENTS FOR SETTLING CHAMBER DISTURBANCES AND THEIR EFFECTS ON TEST SECTION FLOW QUALITY

The only published sources known to this author of information on the existing JPL settling chamber design and flow disturbances are those of Laufer in references 5-7. In reference 5 Laufer states: "The turbulence levels in the settling chamber under the two conditions were 0.6 percent and 7 percent. These values were approximately constant for the Mach number range 1.4 to 4.0, and nearly independent of the tunnel stagnation pressure. The temperature fluctuations were negligibly small." The two conditions just referred to were: (1) when the vorticity fluctuations were reduced by installing damping screens in the settling chamber and, (2) when these disturbances were greatly increased by the installation of a grid before the contraction. The main results of this investigation (ref. 5) were that in the low Mach number flows ($M < 2.5$), the turbulence level of the settling chamber had a strong effect on boundary layer transition Reynolds number but no such effect could be detected for flows at $M > 2.5$. These results agree qualitatively with our own experience here at Langley (ref. 1) where an increase in settling chamber maximum turbulence levels from 0.35 percent to 0.85 percent (this increase was obtained by removing some of the acoustic treatment material) caused no measurable increase in free stream noise levels in the Mach 5 flow. Details of this particular settling chamber design (ref. 1) and techniques used to achieve these low turbulence levels will be discussed in the next section of this report.

Earlier results from an investigation by Westley (ref. 8) of the effect of settling chamber noise on test section noise are of considerable interest to the present discussion. Westley measured the pressure fluctuations with microphones mounted flush with the wall in a blowdown wind tunnel for test section Mach numbers from 1.2 to 4.0. He found intense pressure fluctuations in the settling chamber that apparently originated from the sonic jet of the control valve. He concluded that for $M_\infty < 3$ the pressure fluctuations in the test section were predominately those which had been transmitted from the settling chamber. The attenuation of this transmitted noise increased with increasing M_∞ and for $M_\infty > 3$, the test section noise became almost independent of the settling chamber noise. The reasons for this latter result were that the surface noise and noise radiated from the turbulent boundary layers on the nozzle wall become the dominant disturbance sources at the higher Mach numbers in agreement with Laufer's (refs. 6, 7, and 9) original experiments in the JPL tunnel. In regard to the settling chamber disturbances in these experiments Laufer states (refs. 6 and 7): "The turbulence level in the supply section was found to be due to velocity fluctuations only, no temperature fluctuation being detected. The turbulence level was 1 percent for all Reynolds numbers, except at $M_\infty > 4.5$ where $\tilde{u}/\bar{u}$ = 0.5 percent."

Figure 1 is a schematic diagram of the JPL tunnel taken from reference 6. Note there is a vorticity decay distance of about 2.9 m (9.6 ft.) from the last screen to the inlet of the nozzle contraction. The overall L/D of the main chamber is about 2.3. There are seven 8 x 8 mesh/cm (20 mesh/in.) screens (two of which provide the function of filler screens to prevent separation in the 14° entrance diffuser), a filter paper, and two 12 x 12 mesh/cm (30 mesh/in.) screens. Whether more screens were added for the investigation of reference 5 to get the reported lower 0.6 percent turbulence level is not known. For the purposes of this discussion, it may be assumed that the different turbulence levels of 0.6 and 1 percent were due to variations in operating conditions or instrumentation accuracy. Some fraction of the nominal 1 percent turbulence level in these tests was probably due to acoustic disturbances which originate primarily from upstream sources. These upstream acoustic sources are peculiar to each wind tunnel drive system and duct or piping system, including its valves and physical layout. In particular, it is well known that typical blowdown wind tunnels have extremely high noise levels over wide frequency spectra that are caused by the piping system, the pressure reducing valves, and the pressure control valves. These severe noise problems and proven methods of achieving very significant attenuation of the settling chamber input levels will be discussed in the next section of this report.

Returning to the vorticity disturbance problem, in order to evaluate the performance of the existing turbulence screens in the JPL tunnel, the range of pertinent flow conditions in the settling chamber and test section (based partly on data from ref. 10) are given in Table I for T_o = 294K (530°R). Since the mass flow rates, for a given value of T_o, are directly proportional to p_o, a comparison of the maximum values of p_o in Table I with the new proposed values (PER) shows that the new mass flows will be more than doubled over the entire Mach number range. This increase in mass flow will not affect the settling chamber velocities or Mach numbers but will more than double the screen Reynolds numbers.

From Table I(b), it is of interest to note that when the nozzle wall boundary layer was laminar, which results in ultra-quiet test section flow (see ref. 1), the maximum values of $R_{sc} \simeq 185$/cm (470/inch) would give a screen wire diameter Reynolds number of only 4.7 for d = .25 mm (.01 inch). This value of $R_{sc,d}$ is far below the critical range of approximately 40 for which a screen will just begin to generate new turbulence due to transition from laminar to turbulent flow in the wire wakes. That is, for these very low, subcritical screen Reynolds numbers, the wire wakes are laminar which presumably would contribute to the maintenance of the observed laminar boundary layers on the nozzle walls at the conditions of Table I(b).

The main parameters used to assess the performance of turbulence damping screens are the porosity β (or solidity $\sigma = 1 - \beta$), the mesh m, wire diameter d, and Reynolds numbers based on these dimensions. Values of these parameters for two typical screens are given in Table II for conditions in the existing JPL tunnel and in the new modified tunnel (PER). Note that the solidity of the proposed 8 x 8 mesh/cm (20 x 20 mesh per inch) screen is somewhat larger than the recommended limit of about 0.42 (refs. 11 and 12) which is required to avoid anomalous increases of vorticity due to random merging of some of the screen wire wakes. Also note from Table II that the maximum values of $R_{sc,d}$ for both the existing JPL tunnel and the modified version are far above the critical value of about 50 (refs. 11 and 12) so that new higher turbulence would be generated by each screen. However, from results in references 11 and 12, the turbulence far downstream for $x/m \geq 200$ was always lower than the input values, so presumably, if sufficient decay distance is provided downstream of each screen, the final decay turbulence levels would always be lower than input levels in spite of the supercritical Reynolds numbers. The question then arises as to what the minimum spacing between multiple screens should be. Tests of multiple screens reported in reference 12 with $\Delta x/m$ values from only 9.4 to 30.3 showed that the overall turbulence reduction factor was

$$F_n = (1 + K)^{-n/2.7} \tag{1}$$

where n is the number of successive screens in series and K is the pressure drop coefficient of a single screen. Their exponent of n/2.7 was smaller (which results in less turbulence reduction) than the classical value of n/2 from Dryden and Schubauer (ref. 13) possibly because the levels of turbulence in their input flow were thought to be higher than in the tunnel of Dryden and Schubauer. However, another important factor that affects the decay distances is the screen Reynolds numbers. Increasing decay distances are generally required as the screen Reynolds numbers are increased, especially up to the critical value of $R_{sc,d} \simeq 50$ (ref. 11). For the much larger screen Reynolds numbers in Table II, it seems prudent to specify distances between screens of $\Delta x/m \simeq 100$ or larger if possible. (Note that the minimum spacing between screens in the existing JPL tunnel is $\Delta x/m \simeq 180$ (see fig. 1).)

The overall effectiveness of multiple screens is increased by minimizing any swirl or nonuniformities in the approaching mean flow. The use of a

honeycomb with an additional matching screen just downstream of it are usually effective for this purpose (refs. 14 and 15). The optimum ℓ/m (where m is the honeycomb mesh size) is about 8 although this is apparently not critical. To approach asymptotic decay of new turbulence downstream of a honeycomb, it should be placed upstream of the first damping screen by about 50 honeycomb mesh distances (ref. 14).

For large diameter, high dynamic pressure settling chambers, the pressure loads on honeycombs and screens must be accurately known. For honeycombs with hexagon cells, a good source of data is reference 15. From a plot of their experimental values of K against $R_{sc,m}$ and by interpolation for $\ell/m \simeq 8$, the following relation is obtained:

$$K = 197\left(R_{sc,m}\right)^{-.716} \quad ; \quad \ell/m \approx 8 \tag{2}$$

For damping screens at high Reynolds numbers, Laws and Livesey (ref. 16) give the following relation:

$$K = 0.52\,\frac{1-\beta^2}{\beta^2} \tag{3}$$

With these equations and flow data like those in Tables I and II, the loads on honeycombs and screens may be computed with good accuracy. If conventional screens will not take the loads in a high q, large settling chamber, then honeycombs, perhaps even 2 or 3 in series, with decreasing mesh sizes in the downstream direction, would have to be used.

To conclude this section, it seems clear that rms velocity fluctuation levels (which include both vorticity and acoustic disturbances) at the settling chamber exit just upstream of the nozzle contraction should be reduced to 1 percent or less, particularly for operation at the lower Mach numbers below 3. To achieve this low level of turbulence, screen solidities of less than 0.42 should be used and 5 to 7 damping screens in series placed at least 100 mesh distances apart will probably be required. A honeycomb and an additional matching screen (ref. 14) placed upstream of the damping screens by about 50 honeycomb mesh distances will minimize any swirl or other mean flow nonuniformities and increase the effectiveness of the damping screens.

However, the damping screens and honeycombs will not attenuate the high level and high frequency acoustic disturbances that are typical of blowdown systems. Thus, in order to meet the requirement of 1 per cent turbulence or less in terms of the total velocity fluctuation levels, the acoustic disturbances must also be reduced to very low levels, particularly for test section Mach numbers below about 3. Proven and comparatively simple ways of reducing the acoustic disturbances will be discussed in the next section.

REDUCTION OF ACOUSTIC DISTURBANCES IN BLOWDOWN WIND TUNNELS

We will now consider the problem of how to reduce the high level, broadband acoustic disturbances in blowdown wind tunnels to the low levels required to achieve 1 percent total turbulence or less in the settling chamber. The

design engineer must also address the equally important problem of how to achieve these required low noise levels with the minimum cost as determined by settling chamber length, diameter, and the type of acoustic baffles or other acoustic treatment components.

First a brief discussion of measurement techniques and data interpretation will be offered to help clarify certain arguments presented in the following sections. The basic relation between rms pressure and particle velocity amplitudes in a plane sound wave is (ref. 17)

$$\tilde{p} = \rho c \tilde{u} \tag{4}$$

thus

$$\frac{\tilde{p}}{\bar{p}} = \gamma M \frac{\tilde{u}}{\bar{u}} \tag{5}$$

since $M = \bar{u}/c$ and $c = \gamma \bar{p}/\bar{\rho}$. This relation has been used (refs. 1 and 18) to express hot-wire data obtained in the low velocity settling chamber flows in terms of pressure fluctuations. The purpose of this conversion of hot-wire data is to provide a comparison with pressure fluctuation measurements obtained from pressure transducers mounted flush with the wall (ref. 18) or in probes used within the settling chamber flow itself (ref. 19). Such a comparison between hot-wire and pressure transducer data provide an estimate of the relative contributions of acoustic and vorticity disturbances to the total turbulence by invoking several assumptions (refs. 18 and 19). Three of these assumptions are: (1) the acoustic disturbance is a plane wave moving axially along the chamber, (2) the contribution to the hot-wire signal due to density fluctuations can be neglected, and (3) if the transducer is flush mounted on the chamber wall, the turbulent boundary layer surface noise (or "pseudo" sound) is either previously known (from data correlations in noise free environments) or is much smaller than the free stream noise. In addition, the entropy fluctuations (or temperature spottiness) must be negligible which is usually the case in unheated flows or when thorough mixing of the flow is provided. As will be seen, this required mixing can be accomplished by suitable settling chamber components. In low speed flows, the density fluctuations are usually neglected, even when the acoustic disturbances are large.

The justification for neglecting the density fluctuations is as follows: The probe wire current or voltage (for a constant temperature wire) is proportional to the square root of the aerodynamic heat transfer rate to the wire that, in turn, is proportional to the mass flow per unit area, ρu, at a given mean flow condition. The mass flow fluctuations may be expressed in terms of differential quantities as

$$\frac{d\dot{m}}{\dot{m}} = \frac{du}{\bar{u}} + \frac{d\rho}{\bar{\rho}} \tag{6}$$

Since vorticity fluctuations are, by definition, pure velocity fluctuations, equation (6) may be separated into acoustic and vortical components and written as

$$\frac{d\dot{m}}{\dot{m}} = \left(\frac{du}{\bar{u}}\right)_a + \left(\frac{d\rho}{\bar{\rho}}\right)_a + \left(\frac{du}{\bar{u}}\right)_v \tag{7}$$

Then since the acoustic density fluctuations are isentropic,

$$\left(\frac{d\rho}{\bar{\rho}}\right)_a = \frac{1}{\gamma}\left(\frac{dp}{\bar{p}}\right)_a$$

equation (5) may be written as (where, for the present purposes, the differential notation is fully equivalent to the rms notation)

$$\left(\frac{d\rho}{\bar{\rho}}\right)_a = M\left(\frac{du}{\bar{u}}\right)_a \tag{8}$$

Equation (7) then becomes

$$\frac{d\dot{m}}{\dot{m}} = (1+M)\left(\frac{du}{\bar{u}}\right)_a + \left(\frac{du}{\bar{u}}\right)_v \tag{9}$$

Thus, for $M \ll 1.0$, equation (9) takes the form

$$\frac{d\dot{m}}{\dot{m}} = \left(\frac{du}{\bar{u}}\right)_a + \left(\frac{du}{\bar{u}}\right)_v \tag{10}$$

It is now clear from this result that if an independent measurement of the acoustic velocity contribution is available by using equation (5) with $\tilde{p}/\bar{p}$ supplied by a pressure transducer and if the total velocity fluctuations are obtained from hot-wire data (eq. (10)), then the vorticity contribution can be evaluated subject to the limitations discussed above.

Settling Chamber for Mach 5 Pilot Quiet Tunnel

The first example of very significant acoustic noise reduction and the evaluation of relative acoustic and vortical disturbances in a settling chamber is taken from reference 18. Figure 2 shows the basic data for $\tilde{u}/\bar{u}$ from the hot-wire probe on the centerline and the corresponding values of $\tilde{p}/\bar{p}$ from equation (5) are plotted on the same scale with the pressure transducer data in the bottom portion of the figure. In this case, the turbulent boundary layer wall noise may be calculated from the relation

$$\frac{\tilde{p}_w}{\bar{p}} = \frac{\tilde{p}_w}{q_{sc}} \frac{\gamma}{2} M_{sc}^2 \tag{11}$$

where $\frac{\tilde{p}_w}{q_{sc}} \approx .006$ from reference 20 (for $M \leq .01$) and $M_{sc} = .0066$ based on the settling chamber and nozzle throat (with bleed valves open) cross-sectional areas (ref. 1). The resulting value of $\tilde{p}/\bar{p} \approx 1.8 \times 10^{-7}$ which is about two orders of magnitude smaller than the pressure transducer data shown in figure 2. Since the reduced hot-wire data are in close agreement with the pressure data, we can therefore conclude that the vorticity fluctuations in

this settling chamber are indeed small. Note, however, that due to accuracy limitations of both techniques as well as limitations imposed by the previously mentioned assumptions, no particular significance should be attached to the apparent result that the reduced hot-wire data are lower than the pressure data. Nevertheless, it is clear that the already remarkably low turbulence levels of 0.2 to 0.4 percent shown in the upper part of figure 2 are mostly acoustic disturbances. The hot-wire spectra data published in reference 1 are consistent with this conclusion because significant energy was present up to at least 40 kHz which could not possibly be vorticity with the low stream velocities of about 2.5 m/sec (8 ft./sec) in this chamber.

In order to appreciate the large amount of acoustic attenuation realized in this settling chamber, the wall pressure fluctuations measured at the inlet are shown in figure 3 taken from reference 1. The peak levels are about 4×10^{-3} or two orders of magnitude larger than the values measured downstream of the acoustic baffle components. Before presenting a description of these acoustic components and some information about the very effective turbulence screens in this chamber, some comments are in order concerning the large decrease in the inlet noise levels with increasing unit Reynolds number starting at $R_{sc} \approx 10^6$/m (fig. 3).

A schematic sketch of the upstream supply piping system for this tunnel is shown in figure 4. The two control valves are located downstream of the 25.4 cm (10 inch) header or large supply pipe which is always pressurized to about 3800 kPa (550 psia) by reducing valves from the main high pressure air storage tanks. For the relatively small mass flows in this Mach 5 Pilot Quiet Tunnel of about 3.9 kg/sec (8.6 lb/sec) maximum (for the tests of fig. 2), the header functions essentially as a static air tank. To obtain the largest unit Reynolds number shown in figure 3, the 10.2 cm (4 inch) valve was nearly wide open with a ratio of downstream to upstream pressure of about 0.55. Thus, the flow through the valve at the higher pressures is subsonic, or unchoked, with much smaller noise emission, while at the lower unit Reynolds numbers, the valve flow is always sonic, or choked, with corresponding high noise levels. Again the spectral data shown in reference 1 are consistent with this flow noise assessment. However, even with the valve wide open, the remaining inlet pipe noise is still nearly an order of magnitude higher than the levels in the settling chamber downstream of the acoustic components (fig. 2). Thus, the inherent pipe noise even in this fairly simple system would be too large to be acceptable for a supersonic blowdown wind tunnel with the required flow quality for $M_\infty < 3$.

It is of interest to compare the pipe and settling chamber noise levels in the Mach 5 Pilot Quiet Tunnel with those in the Vought Systems Division 4 x 4 ft. transonic and supersonic blowdown wind tunnel (ref. 21). The control valve (cylindrical-rotor type valve) in the Vought tunnel was immediately upstream of the inlet diffuser to the settling chamber. The diffuser expanded the sonic valve flow to high supersonic velocities which terminated through a normal shock system resulting in very high noise levels of $\tilde{p}/\bar{p} \approx 1$ percent in the settling chamber. Four perforated plates were then installed in the diffuser and the settling chamber noise was reduced to $\tilde{p}/\bar{p} \approx 0.3$ percent by a system of multiple shocks rather than the terminal normal shock system. This reduced level is about the same as the peak inlet values in figure 3 for the Mach 5 Pilot Quiet Tunnel. These latter values

were then further reduced by two orders of magnitude by the settling chamber components in the Mach 5 Pilot Quiet Tunnel. Obviously, the inlet flow mechanisms are entirely different in the two facilities.

The Lockheed 4-foot blowdown wind tunnel (ref. 22) had originally the same design as the Vought tunnel and therefore experienced the same severe noise problems due to the rotor type control valve and inlet diffuser. An extensive development program to improve the flow quality in this tunnel was carried out with a 1/2 scale model and the results are given in reference 22. Data were obtained with the cylindrical-rotor valve replaced with two different sleeve valves; one was designed to give the required pressure drop with multiple small shocks while the other valve had numerous (5,550), small, tortuous air passages in its sleeve designed to generate pressure losses through a series of subsonic flow turns rather than through shocks. This latter valve is typical of so-called "quiet" valves and, when used with no other flow conditioners, it did reduce the normalized rms noise from a maximum level of $\tilde{p}/\bar{p} \approx 2$ percent (caused by the rotor valve) to about 0.3 percent. This reduced level is again about the same as the peak input levels for the Mach 5 Pilot Quiet Tunnel (fig. 3). With the addition of several flow conditioners consisting of three filling grids to prevent separation in the large angle inlet diffuser, a honeycomb, and four damping screens, the minimum noise level downstream of all conditioners was reduced to $\tilde{p}/\bar{p} \approx 0.08$ percent which is still more than an order of magnitude larger than in the small chamber (fig. 2). It is doubtful whether this particular quiet valve design would provide any significant attenuation of high level and high frequency pipe noise such as would be present in the existing Langley complex, especially at high mass flow rates. Additional details on the sources and characteristics of this pipe noise will be discussed in the next section of this report.

Data reported in reference 1 show that most of the acoustic attenuation in the small settling chamber for the Mach 5 Pilot Quiet Tunnel was provided by two porous ("Rigimesh") components and a section of steel wool that was 8.9 cm (3.5 in.) in streamwise length. These components and other details of this chamber are shown in figure 5. The overall pressure drop for all acoustic components and damping screens is given by

$$\frac{\Delta p}{p_o} \approx .09 + \frac{2.2}{p_o} \quad ; \quad p_o > 30 \text{ psi} \tag{12}$$

where, in the last term, p_o is in psia. For comparison with other data this equation may be written in terms of the pressure drop coefficient as

$$K \approx \frac{.09}{\frac{\gamma}{2} M_{sc}^2} + \frac{2.2}{\frac{\gamma}{2} p_o M_{sc}^2} \tag{13}$$

This result shows that (for $p_o > 30$ psia) the value of K decreases with increasing Reynolds number since for constant values of T_o and M_{sc}, the Reynolds number is proportional to p_o.

The entrance baffle (or entrance jet "diffuser") was either the porous hemisphere or the porous cone as indicated in figure 5. Data reported in reference 1 shows that the downstream rms velocity levels on the centerline were approximately the same for these two entrance baffles. However, the cone was generally preferred over the hemisphere because of the somewhat greater attenuation of the acoustic energy at high frequencies above 15 kHz (ref. 1). The hemisphere is no longer used but did produce a somewhat more uniform distribution of $\tilde{u}/\bar{u}$ across the chamber as indicated by the hot-wire data shown in figure 6. The data for the hemisphere at $r = 0$ (on the centerline) are the same as the hot-wire data shown in figure 2. The off-centerline data in figure 6 have not been published before.* It is of interest to note that even though these hot-wire data were measured far downstream of all acoustic components and damping screens, the shape of the upstream porous entrance baffle could apparently influence the turbulence distribution to the extent shown in figure 6. Due to a lack of systematic investigation, insufficient data are available to determine whether the nonuniform distributions of $\tilde{u}/\bar{u}$ with the cone were repeatable and actually caused by the conical shape or were due to local aberrations in the cone porosity. For the same reason, the precise contributions of the fairly high porosity (β = 57 percent) perforated plate and the particular sequence of mesh sizes of the damping screens, to the low levels of turbulence is not known. More detailed data in a larger settling chamber to be discussed in the next section will provide some indication of what nonuniform porosities and high solidity perforated plates can do to the downstream flow.

Before proceeding to this next and last example of large noise attenuation in the settling chamber of a blowdown wind tunnel, one final but very important point will be made about the chamber for the Mach 5 Pilot Tunnel. The methods of mounting the damping screens and installing them in the chamber are considered to be of unusually high quality. With several years of use and frequent cleaning the screens have been easily maintained in the ideal taut condition and free of any defects. The engineering design details of this installation are available upon request. The range of wire diameter and mesh size Reynolds numbers for the downstream 20 x 20 mesh/cm (50 mesh/in.) screens corresponding to the conditions of figure 6 are $R_{sc,m}$ = 65 to 1400 and $R_{sc,d}$ = 15 to 300. Thus, the screens were operated over the entire range from subcritical to supercritical wire diameter Reynolds numbers. However, the streamwise spacing between these downstream 20 x 20 mesh/cm screens was probably more than sufficient at $\Delta x/m \simeq 200$ to allow asymptotic decay of the generated vorticity (refs. 11 and 12). The solidity of the 20 x 20 mesh/cm screens was $\sigma = .40$ which is below the recommended limit of $\sigma = .42$ (refs. 11 and 12).

*The author is indebted to J. B. Anders of NASA Langley for supplying these data on figure 6.

Settling Chamber for the Supersonic Pilot Quiet Tunnel

Figure 7 is a schematic scale drawing of the large settling chamber for the Supersonic Pilot Quiet Tunnel. This chamber is 60.1 cm (23.66 in.) in diameter by 6.4 m (20.9 ft.) long and was originally equipped with 5 porous Rigimesh components and 7 damping screens as illustrated in the figure. The entrance baffle is a porous Rigimesh cone and the four Rigimesh plates are contoured to an arc radius of 60 cm (23.7 in.) in the downstream direction, as illustrated, to reduce stresses on the material. The spacing between the contoured plates, starting at the upstream space, is 41.3 cm (16.2 in.), 34.9 cm (13.8 in.), and 37.7 cm (14.8 in.). The upstream space is packed tightly with coarse steel wool. The throat diameter of the nozzle at the settling chamber exit was 10.160 cm (4.000 in.). This nozzle was used for all test results reported herein.

If the mean flow through the nozzle throat is uniform and sonic, the mass flow in the settling chamber is

$$\dot{m}_{sc} = \left(\frac{\gamma+1}{2}\right)^{-\frac{\gamma+1}{2(\gamma-1)}} \sqrt{\frac{\gamma}{\bar{R}}} \quad \frac{p_o A_*}{\sqrt{T_o}} \tag{14}$$

where A_* is the effective throat area which may include a correction for the boundary layer displacement thickness. If the mean flow in the settling chamber is uniform the Mach number and velocity then follow from eq. (14) as

$$M_{sc} = \left(\frac{\gamma+1}{2}\right)^{-\frac{\gamma+1}{2(\gamma-1)}} \quad \frac{A_*}{A_{sc}} \tag{15}$$

$$\bar{u}_{sc} = \left(\frac{\gamma+1}{2}\right)^{-\frac{\gamma+1}{2(\gamma-1)}} \sqrt{\gamma \bar{R} T_o} \quad \frac{A_*}{A_{sc}} \tag{16}$$

where the speed of sound in the settling chamber is assumed to be $c_{sc} = \sqrt{\gamma \bar{R} T_o}$ and A_{sc} may again include a correction for the local boundary layer displacement thickness. The inviscid values of Mach number and velocity from these equations are $M_{sc} = .0165$ and $\bar{u}_{sc} = 5.8$ m/sec (19.2 ft/sec) for $T_o = 310$ K (560°R).

Results of a detailed investigation of the flow in this settling chamber with hot-wire probes will be available.* The distribution across the chamber at ports A, B, and D of mean and fluctuating velocities, including spectral data and analysis, with various combinations of the porous components shown

*To be published as an NASA CR by Michael J. Piatt, Systems and Applied Sciences Corporation.

in figure 7, and with the addition of a high density perforated plate and a honeycomb will be included. Fluctuating pressure data, including spectral measurements, obtained with high frequency response transducers mounted flush with the wall at port D will also be available.*

Noise attenuation and centerline turbulence. - Figure 8 compares data from these sources with pressure and hot-wire data in the settling chamber of the Mach 5 Pilot Quiet Tunnel from figure 2. Several important conclusions can be obtained from this figure. First, figure 8(a) shows that the normalized rms acoustic pressure fluctuations in the large chamber for $f > 20$ Hz with all components installed follow the same trend with unit Reynolds number as in the Mach 5 chamber except for the decrease at $R_{sc}/m \approx 10^6$ caused by the unchoked control valve flow in the Mach 5 facility discussed previously. Thus, if the unit Reynolds number is the correlating parameter for acoustic attenuation by high Δp porous plates, then values of $\tilde{p}_w/\bar{p}_o$ .006 percent should be possible in the modified JPL tunnel since the maximum value of unit Reynolds number in the 2.44 m (8 ft.) diameter settling chamber will be about 1.7×10^6/m. Second, the levels of $\tilde{p}_w/\bar{p}_o$ in the large chamber with all components removed (considered equivalent to values at the chamber inlet) are about 0.2 percent which is smaller than the peak inlet levels in the small chamber from figure 3. Thus, even though the piping systems and mass flows are drastically different for these two facilities (details of the piping system for the Supersonic Pilot Quiet Tunnel will be given in Keyes' report), the levels of $\tilde{p}/\bar{p}_o$ at the inlet and downstream of the porous components are similar in magnitude. In both chambers, the entrance baffle not only prevents separation of the inlet jet but also provides some attenuation of the pipe noise.

On the other hand, comparison of the hot-wire data for centerline velocity fluctuations given in figure 8(b) shows that the total turbulence levels in the large chamber are more than twice the corresponding turbulence levels in the small chamber. Furthermore, comparison of the hot-wire and pressure transducer data for the large chamber in figure 8(b) shows that these increased turbulence levels are primarily due to increases in vorticity fluctuations based on the previous discussion and equation (10). Another important result from figure 8 is the significantly large energy in the pressure fluctuations at low frequencies for $f < 20$ Hz as indicated by comparison of the two bands of pressure data at the two different electronic filter settings with all components installed.

This low frequency energy was initially believed to be caused by oscillations in the pressure control valves. To investigate this possibility and to determine if lower noise levels would occur if the control valves were operated wide open, a special set of runs was made with the high pressure tank field bled down to pressures much lower than the normal range. The results are shown in figure 8(c) where data for both frequency filter settings and normal operation of the control valves are included for comparison. The data for $f = 0 - 70{,}000$ Hz (left side of the figure) show that some of the low frequency energy does come from the control valves

*To be published as an NASA TP by J. Wayne Keyes, NASA Langley.

since the levels are somewhat lower with the valves wide open. When $f < 20$ Hz is filtered out (right side of figure) there is very little difference in noise levels between normal operation and wide open settings of the control valves. In view of the high level valve noise for the small chamber shown in figure 3 and also apparent in figure 2 from the decrease in $\tilde{p}/p_o$ for $R_{sc}/m > 10^6$, this lack of any valve noise for the large chamber system came as a big surprise. The explanation is probably to be found in the very high "pipe" noise due to tees, reducers, elbows, etc., that now becomes dominant because of the much higher mass flows, up to about 55 kg/sec (120 lb/sec), during these tests. Furthermore, this inherent pipe noise is not affected much by flow through the heater since bypassing the heater did not affect the measured noise levels appreciably. It must be concluded that at the much higher mass flows of 130 kg/sec (280 lb/sec) for the modified JPL tunnel installation in this same facility complex, the pipe noise sources will predominate over any other control valve or reducing valve noise sources. Thus, the proposed quiet control valve may not reduce the noise levels at the settling chamber inlet appreciably since the very high intensity and high frequency pipe noise will probably be transmitted directly through it, unless the internal components and acoustic control devices are tailored to match this input noise.

The large values of pressure drop across the porous components in this chamber and the effects on Δp of foreign material stopped by the components are illustrated in figure 9. The increasing values of Δp with increasing number of runs were caused primarily by material from the disentegration of the Balston filter elements made of fiber glass and epoxy bonding that were originally installed upstream of the settling chamber. The failure of these elements was probably caused primarily by the high energy, low frequency noise or oscillations in the flow (fig. 8). Most of this filter material was retained by the entrance cone. The purposes of the upstream filter were to keep the porous components free from contamination, to protect the surface finish of highly polished nozzles or models from pitting and erosion, and finally to prevent damage to delicate hot-wire probes and pitot pressure transducers. The Balston filter elements have been replaced with porous stainless steel elements supplied by Pall Trinity. These elements have functioned very well. Fluctuating pressure data obtained at port D with and without filter elements installed showed that the settling chamber noise levels were not affected significantly by the filter elements or their housing.

Figure 10 is a typical power spectrum of the pressure fluctuations at the higher values of R_{sc}/m. This spectrum shows that a significant fraction of the acoustic energy is present over the frequency range from 10 kHz to 55 kHz. The peak at $f \simeq 3$ kHz is apparently caused by structural vibrations transmitted to the mounting plug. The very low frequencies of $f < 20$ Hz are not visible on this figure.

Figure 11 shows the pressure drop across various components or combinations of components plotted against stagnation pressure. These data were obtained before either type of filter elements were installed, so the values (especially for the entrance cone) may be somewhat higher than after cleaning and installation of the Pall filter elements. Nevertheless, it is useful to compare these pressure drop values in terms of K with those in the small chamber.

For the cone alone we obtain from figure 11, for $M_{sc} = .0165$ and for $p >$ 100 psia

$$K = \frac{.14}{\frac{\gamma}{2} M_{sc}^2} + \frac{2}{\frac{\gamma}{2} p_o M_{sc}^2} \tag{17}$$

where here and in the following equation for K, the constant in the last term is in psi. Comparison of equations (17) and (13) shows that the pressure drop coefficient for just the cone is considerably larger than the overall coefficient for the small settling chamber. Similar relations for other combinations may be obtained such as the following equation for K that is applicable to the cone plus 4 plates and 7 screens but without the steel wool:

$$K = \frac{.32}{\frac{\gamma}{2} M_{sc}^2} + \frac{5}{\frac{\gamma}{2} p_o M_{sc}^2} \tag{18}$$

These values of K are much larger than for the small settling chamber, yet the noise attenuation in the big settling chamber is not as large. In the next subsection of this report, test results with the last porous plate removed are presented. Additional results with the steel wool removed and also data without the cone will be available in the Piatt and Keyes reports. The noise attenuation was not affected, within the accuracy of the measurements, by removal of the last porous plate and the steel wool. Therefore, it appears that the original Δp values in the large settling chamber represent an "overkill" approach with more pressure drop than required to achieve the maximum possible noise attenuation. Recalling the highly effective two porous components and 8.9 cm (3.5 in.) of steel wool in the small chamber (fig. 5), a similar arrangement could probably be used in the 2.44 m (8 ft.) diameter settling chamber of the modified JPL tunnel. These porous components in the small chamber are only 0.32 cm (.125 in.) thick with a total pressure drop (to be estimated from eq. (13)) that could perhaps be accommodated in the JPL chamber by the use of a large square cell, say with m ≈ 30 cm (1 ft.), honeycomb type structure welded between the two porous components or between a perforated plate (as in fig. 5) and the downstream porous plate. The critical problem would be the shear loads around the periphery of the assembly, but these loads could be carried partly by the outer part of the honeycomb structure. In any case, the mean and fluctuating velocities can be affected by these individual porous components and one example of this type change will be discussed next.

Typical distributions across the chamber of mean and fluctuating velocities. Figure 12 shows the variations across the large chamber of the mean velocities and $\tilde{u}/\bar{u}$ from hot-wire data at ports A and B with all components shown in figure 7 installed. Figure 12(a) shows extremely nonuniform mean velocity distributions across the chamber at port A that were roughly symmetrical about the centerline. The data at port B shows that the screens are remarkably effective in smoothing this mean velocity distribution. Figure 12(b) shows that the screens reduced the turbulence in the center region from maximum levels of about 16 percent down to about 1 percent.

From previous discussion of figure 8, it is clear that these high turbulence levels upstream of the screens are mainly vorticity fluctuations that probably are caused by the high solidity porous plates.

Based on general results given in references 11 and 12, for example, the large increase in turbulence at port B for $r/r_w \approx 0.7$ may be tentatively attributed to the shear layer in the upstream mean flow at port A. This shear layer is very roughly centered at $r/r_w \approx .7$. The hot-wire spectrum at port B near the peak turbulence region shown in figure 13 tends to confirm that these high turbulence levels are vorticity fluctuations since there is very little energy above 5 kHz in contrast with the pressure spectrum of figure 10. Even 5 kHz represents very small scale vorticity at the small convection velocities shown in figure 12(a).

Data to be reported by Piatt shows the source of the nonuniform mean velocities at port A is not the cone. Tests were then conducted to see if a perforated plate or a honeycomb installed upstream of port A would improve the mean velocity distribution at port A. The perforated plate did not help, probably because its density was too high and it also produced some high intensity tones. The honeycomb was also not effective, either because the radial velocity components were already small or the honeycomb was too close to the screens.

The only "quick fix" attempt that resulted in any significant improvement in turbulence distributions at port B was the removal of the downstream porous plate. Figure 14 shows the results. The mean velocity at port A (fig. 14(a)) is more uniform but nonsymmetrical about the centerline. The turbulence levels (fig. 14(b)) at port A are smaller than with all the porous plates installed (fig. 12(b)). At port B, the turbulence is between 1 and 2 percent and reasonably uniform out to $r/r_w \approx .75$. These levels could probably be reduced by using coarser screens for the upstream locations in the damping screen set or by improving the quality of the screen installation. The porosity of the downstream plate was measured but the results were not consistent with the mean velocity profiles shown in figure 12(a). It was therefore concluded that the mean velocity at port A is determined by the porosity distributions of all the upstream plates acting in concert but with presumably increasingly stronger influences by the downstream plates. Obviously, the porous plates must be as uniform in porosity as possible.

The relatively high turbulence (in this case vorticity) levels of 5 to 7 percent around the outer wall of the chamber at port B (fig. 14(b)) are currently blamed, in part, on the poor screen installation which resulted in steps and roughness on the wall. Plans are now being made to remedy this problem. Another cause of the high wall turbulence (which was well outside the nominal boundary layer edge) is believed to be the welded shear tabs that are used to fasten the porous plates to the settling chamber liners. Improvements in the method of securing the plates to the liner are required.

CONCLUDING REMARKS

The planned operation of the Jet Propulsion Laboratory (JPL) 20-Inch Supersonic Wind Tunnel at NASA Langley as a blowdown tunnel at more than

twice the stagnation pressures and mass flow rates that were used at JPL has prompted a review of fluctuating flow sources, levels, composition, and methods for their reduction and control in the supply section of blowdown wind tunnels. Most blowdown wind tunnels, including those in the facility complex at Langley where the modified JPL tunnel will be installed, experience very high intensity, broadband acoustic disturbances at their settling chamber inlets.

Recent data obtained at Langley show that for high mass flows, these acoustic disturbances originate in the high pressure piping system rather than the control valves. This result suggests that the function of a successful "quiet" control valve would be as an acoustic suppression device for the high level, high frequency inlet noise as well as a passive nongenerator of noise. Measurements in two blowdown tunnels at Langley show that the rms pressure intensity of these inlet disturbances ranges up to about 0.3 percent of the mean stagnation pressures with significant energy out to frequencies of at least 40 kHz. Detailed measurements in the settling chamber of these facilities have shown that these acoustic inputs can be reduced by two orders of magnitude by the use of high pressure drop porous components. One of these components may also function as an entrance jet diffuser and may thereby allow a reduction in the overall length of the settling chamber. The resulting downstream rms pressures, normalized by the stagnation pressure, correlates with the unit Reynolds number in the settling chambers. This result indicates that similar noise reductions should be possible in the modified JPL tunnel at its maximum settling chamber unit Reynolds number which falls in mid-range of the above mentioned correlation.

However, these porous plates generate high level vorticity fluctuations which, fortunately, can be reduced to very low levels by good quality damping screens. The resulting total rms velocity fluctuation levels in the settling chamber have been reduced to 1 percent or less, which is required to insure the specified high quality flow in the test section for Mach numbers below 3 and at high test Reynolds numbers.

Recommendations for suitable mesh sizes, spacing, and pressure drop coefficients for the damping screens and the honeycomb are given based on a review of the literature. Based on the new Langley data, expressions for the pressure drop coefficients for the porous components are also given along with recommendations for the minimum pressure drop required to achieve the two orders of magnitude attenuation in the noise at the settling chamber inlet. A suggestion is also offered for a support configuration consisting of a large cell honeycomb type structure welded between the porous components that could probably withstand the extremely high loads in a large settling chamber. Obviously, detailed stress calculations are required to qualify this approach. A scale model test would also be highly desirable.

REFERENCES

1. Anders, J. B.; Stainback, P. C.; Keefe, L. R.; and Beckwith, I. E.: Fluctuating Disturbances in a Mach 5 Wind Tunnel. Presented at the AIAA Ninth Aerodynamic Testing Conference, Arlington, Texas, June 7-9, 1976. (Available in bound volume of papers.)

2. Beckwith, I. E.: Development of a High Reynolds Number Quiet Tunnel for Transition Research. AIAA Journal, Vol. 13, No. 3, March 1975, pp. 300-306.

3. Harvey, W. D.; Cary, A. M., Jr.; and Harris, J. E.: Experimental and Numerical Investigation of Boundary-Layer Development and Transition on the Walls of a Mach 5 Nozzle. NASA TN D-7976, December 1975.

4. Beckwith, I. E.; Anders, J. B.; Stainback, P. C.; Harvey, W. D.; and Srokowski, A. J.: Progress in the Development of a Mach 5 Quiet Tunnel. Paper presented at the AGARD Symposium on Laminar-Turbulent Transition, AGARD Conference Proceedings No. 224, Copenhagen, Denmark, May 2-4, 1977, pp. 28-1 to 28-14.

5. Laufer, J.: Factors Affecting Transition Reynolds Numbers on Models in Supersonic Wind Tunnels. Journal of Aerospace Sciences, Vol. 21, No. 7, July 1954, pp. 497-498.

6. Laufer, J.: Aerodynamic Noise in Supersonic Wind Tunnels. Progress Report No. 20-378, Jet Prop. Lab., February 27, 1959.

7. Laufer, J.: Aerodynamic Noise in Supersonic Wind Tunnels. Journal Aerospace Aciences, Vol. 28, No. 9, September 1961, pp. 685-692.

8. Westley, R.: Aerodynamic Sound and Pressure Fluctuations in a Supersonic Blowdown Wind Tunnel. NRC of Canada Aero Report LR-274, January 1960.

9. Laufer, J.: Some Statistical Properties of the Pressure Field Radiated by a Turbulent Boundary Layer. The Physics of Fluids, Vol. 7, No. 8, August 1964, pp. 1191-1197.

10. Technical Facilities Catalog. Vol. I NASA NHB 8800.5A(I), October 1974 Edition, p. 6-45.

11. Tan-atichat, J.; Nagib, H. M.; and Loehrke, R. I.: Interaction of Freestream Turbulence With Screens and Grids: A Balance Between Turbulence Scales. To be published in Journal of Fluid Mechanics.

12. Loehrke, R. I.; and Nagib, H. M.: Experiments on Management of Free-stream Turbulence. AGARD Report No. 598, September 1972.

13. Dryden, H. L.; and Schubauer, G. B.: The Use of Damping Screens for the Reduction of Wind Tunnel Turbulence. Journal Aerospace Sciences, Vol. 14, No. 4, April 1947, p. 221.

14. Loehrke, R. I.; and Nagib, N. H.: Control of Free-Stream Turbulence by Means of Honeycombs: A Balance Between Suppression and Generation. Journal of Fluids Engineering, Vol. 98, September 1976, pp. 342-353.

15. Wigeland, R. A.; Ahmed, M.; and Nagib, H. M.: Management of Swirling Flows With Application to Wind Tunnel Design. AIAA Journal, Vol. 16, No. 11, November 1978, pp. 1125-1131.

16. Laws, E. M.; and Livesey, J. L.: Flow Through Screens. Ann. Rev. Fluid Mech. 1978, Vol. 10, pp. 247-266.

17. Kinsler, L. E.; and Frey, A. R.: Fundamentals of Acoustics. John Wiley and Sons, Inc., 1962.

18. Anders, J. B.; Stainback, P. C.; Keefe, L. R.; and Beckwith, I. E.: Sound and Fluctuating Disturbance Measurements in the Settling Chamber and Test Section of a Small, Mach 5 Wind Tunnel. IEEE Publication 75, CHO 993-6AES, September 1975, pp. 329-340.

19. Stainback, P. C.; Anders, J. B.; Harvey, W. D.; Cary, A. M.; and Harris, J. E.: An Investigation of Boundary Layer Transition on the Wall of a Mach 5 Nozzle. AIAA Paper No. 74-136, January 1974.

20. Harvey, W. D.; Bushnell, D. M.; and Beckwith, I. E.: Fluctuating Properties of Turbulent Boundary Layers for Mach Numbers up to 9. NASA TN D-5496, October 1969.

21. Cooksey, J. M.; and Arnold, J. W.: Transonic Flow Quality Improvements in a Blowdown Wind Tunnel. J. Aircraft, Vol. 10, No. 9, September 1973, pp. 554-560.

22. Whitfield, E. L.: Noise and Flow Management in Blowdown Wind Tunnels. AGARD-CP-174, March 1976, pp. 6-1 to 6-8.

TABLE I.- FLOW CONDITIONS IN EXISTING JPL 20-INCH SWT, T_o = 294 K (530° R)

(a) Nominal ranges of settling chamber and test section conditions.
Based on reference 10.

M_∞	p_o range kPa (psia)		$\frac{A_{sc}}{A^*}$	M_{sc}	$\bar{u}_{sc}$ m/sec (ft./sec)	R_{sc} range per m (per in.)		q_{sc} range Pa (lb/ft^2)		R_∞ range per m	
0.4	27.6	103	–	.018	6.22	1.12 E 5	4.17 E 5	6.32	23.70	2.30 E 6	8.63 E 6
	(4.00)	(15)			(20.42)	(2.84 E 3)	(1.06 E 4)	(1.32 E -1)	(4.95 E -1)		
1.4	.34	152	22.42	.026	8.88	1.99 E 3	8.78 E 5	.16	70.86	5.23 E 4	2.30 E 7
	(.05)	(22)			(29.13)	(5.06 E 1)	(2.23 E 4)	(3.36 E -3)	(1.48 E 0)		
2.0	.34	193	33.94	.017	5.86	1.31 E 3	7.36 E 5	.070	39.26	4.32 E 4	2.42 E 7
	(.05)	(28)			(19.24)	(3.34 E 1)	(1.87 E 4)	(1.47 E -3)	(8.20 E -1		
3.0	6.21	193	85.15	.0068	2.34	9.45 E 3	2.93 E 5	.201	6.22	4.73 E 5	1.47 E 7
	(.90)	(28)			(7.67)	(2.40 E 2)	(7.45 E 3)	(4.19 E -3)	(1.30 E -1)		
4.0	11.9	317	215.5	.0027	.92	7.13 E 3	1.91 E 5	.060	1.60	5.49 E 5	1.47 E 7
	(1.72)	(46)			(3.03)	(1.81 E 2)	(4.84 E 3)	(1.25 E -3)	(3.34 E -2)		
5.0	27.6	421	502.7	.0012	.40	7.09 E 3	1.08 E 5	.026	.390	8.26 E 5	1.26 E 7
	(4.00)	(61)			(1.30)	(1.80 E 2)	(2.75 E 3)	(5.34 E -4)	(8.14 E -3)		

(b) Conditions with laminar boundary layer on nozzle wall.*

M_∞	p_o		$\frac{A_{sc}}{A^*}$	M_{sc}	$\bar{u}_{sc}$		R_{sc}		q_{sc}		R_∞	
	kPa	psia			m/sec	ft/sec	per m	per in.	Pa	lb/ft^2	per m	per in.
2.40	6.9	1.00	48.32	.012	4.12	13.51	1.85 E 4	4.69 E 2	0.694	1.45 E -2	7.16 E 5	1.82 E 4
3.75	16.6	2.40	171.9	.0034	1.16	3.80	1.24 E 4	3.16 E 2	.131	2.74 E -3	8.64 E 5	2.19 E 4
4.50	46.5	6.75	333.0	.0017	.60	1.96	1.81 E 4	4.59 E 2	.098	2.05 E -3	1.72 E 6	4.37 E 4

*Private communication with J. M. Kendall of J.P.L., Oct., 1979.

TABLE II.- TYPICAL DAMPING SCREEN PARAMETERS

Mesh per cm (per in.)	d mm (in.)	m mm (in.)	β	σ[1]	R_{sc}/m			$R_{sc,d}$			$R_{sc,m}$			Max. laminar Table I(b), $M_\infty = 2.4$	
					JPL min[2]	JPL max[3]	New max[4]	(2)	(3)	(4)	(2)	(3)	(4)	$R_{sc,d}$	$R_{sc,m}$
8 × 8	.33	1.27	0.55	0.45	1.3 E 3	8.8 E 5	1.7 E 6	0.43	290	553	1.67	1120	2130	6.1	23.5
(20 × 20)	(.013)	(.050)													
12 × 12	.18	.84	.62	.38	1.3 E 3	8.8 E 5	1.7 E 6	.23	156	298	1.10	736	1400	3.3	15.5
(30 × 30)	(.007)	(.033)													

(1) $\sigma \leq 0.42$ recommended limit, but $\sigma \approx 0.3$ is better (Ref. 11).

(2) At $M_\infty = 2.0$ (Table I(a)).

(3) At $M_\infty = 1.4$ (Table I(a)).

(4) At $M_\infty = 1.4$, $p_o = 290$ k Pa (42 psia), $(R_{sc}/m) \approx 1.68 \times 10^6$ (PER)

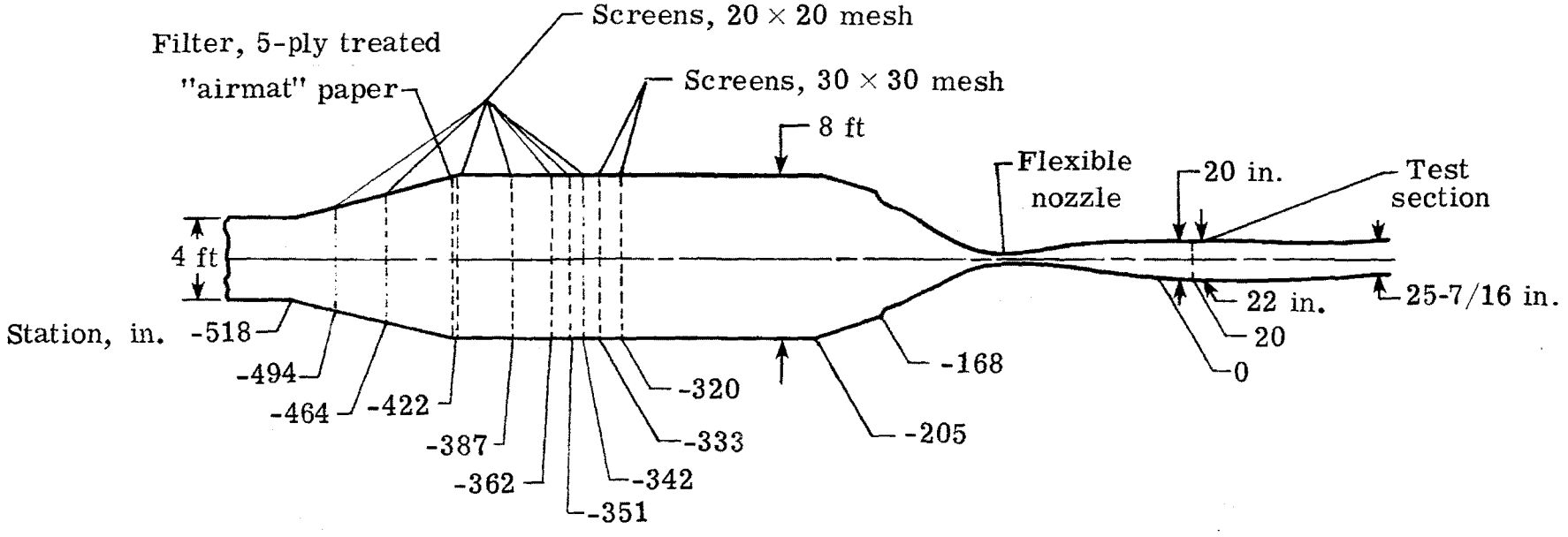

Figure 1.- Schematic diagram of the JPL 20-inch Supersonic Wind Tunnel (from ref. 6).

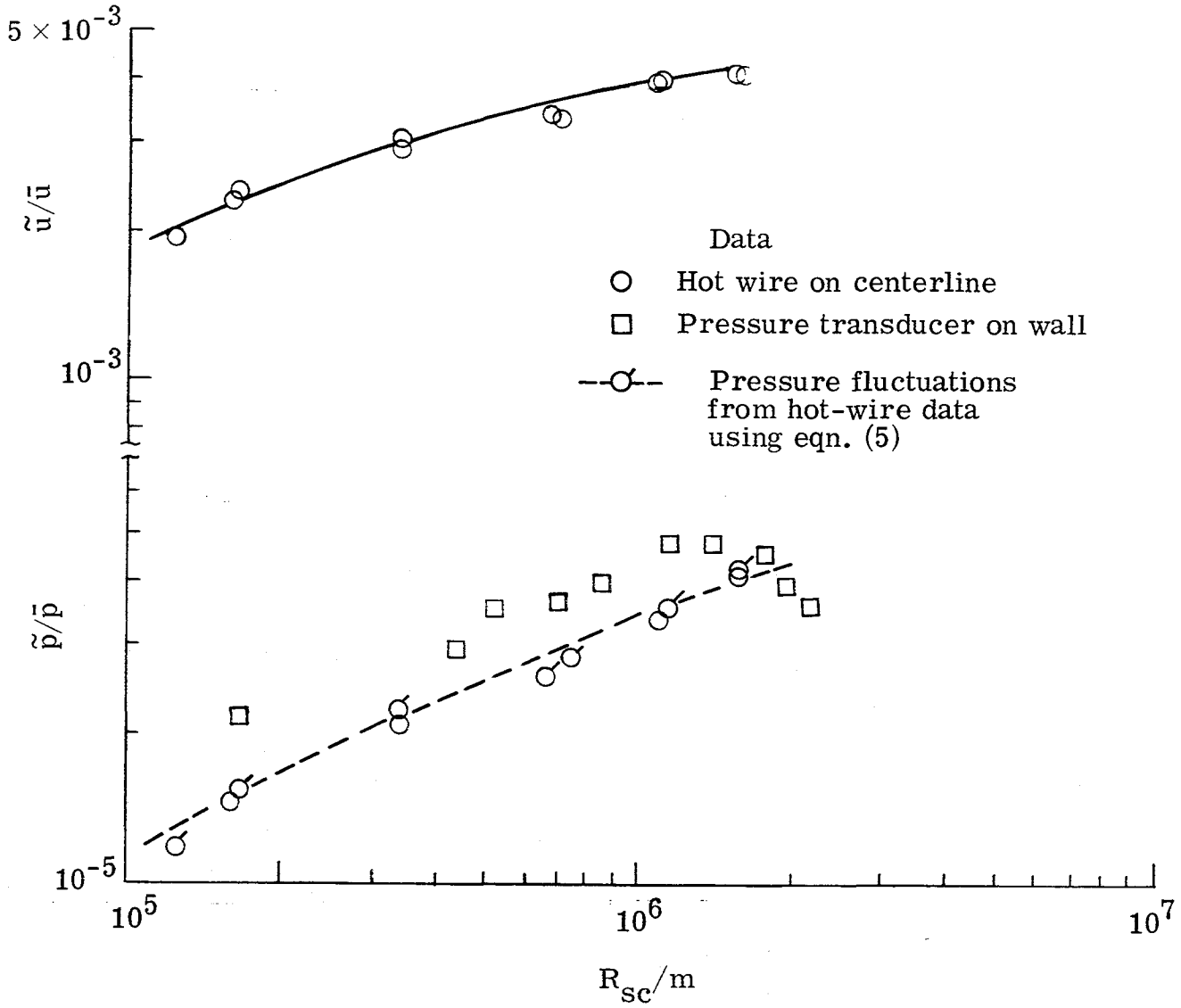

Figure 2.- Velocity and pressure fluctuations just upstream of nozzle contraction in settling chamber of Mach 5 Pilot Quiet Tunnel (ref. 18).

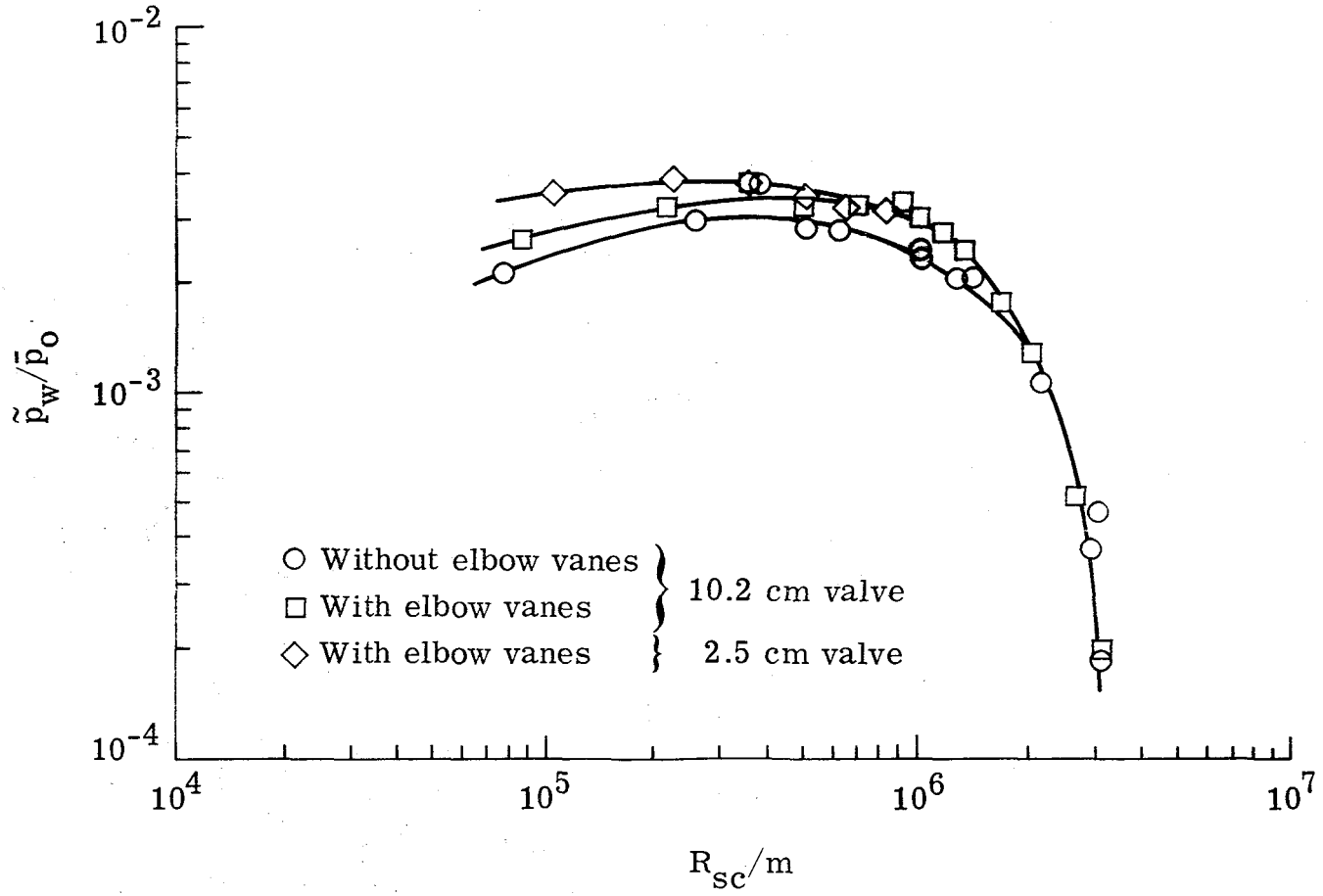

Figure 3.- Wall pressure fluctuations at settling chamber entrance of Mach 5 Pilot Quiet Tunnel (ref. 1).

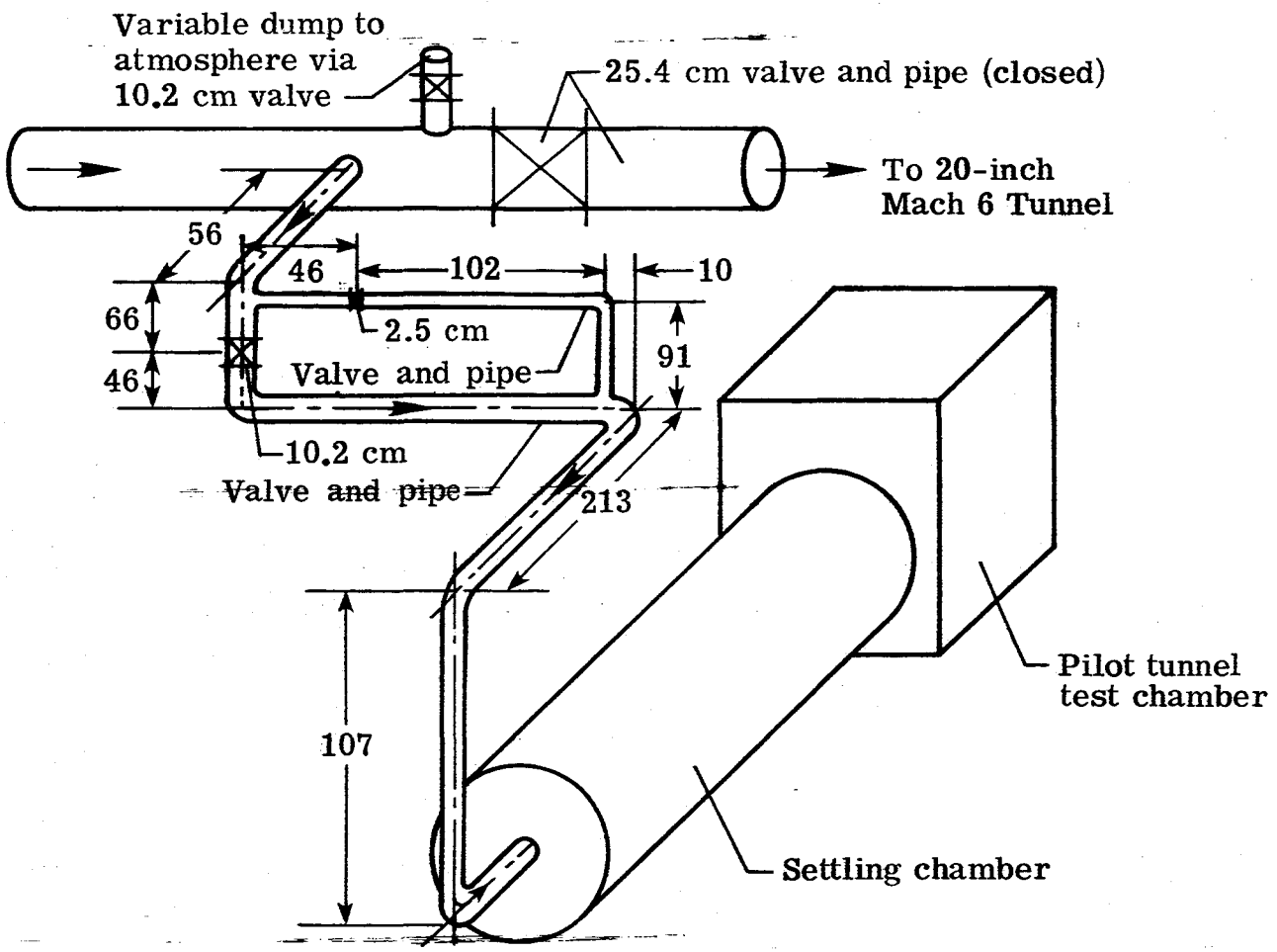

Figure 4.- Schematic sketch of piping for Mach 5 Pilot Quiet Tunnel (ref. 1). Pressure in 25.4 cm pipe maintained at 350 to 400 N/cm^2 (500 to 600 psia) for all tests. (Dimensions in cm.)

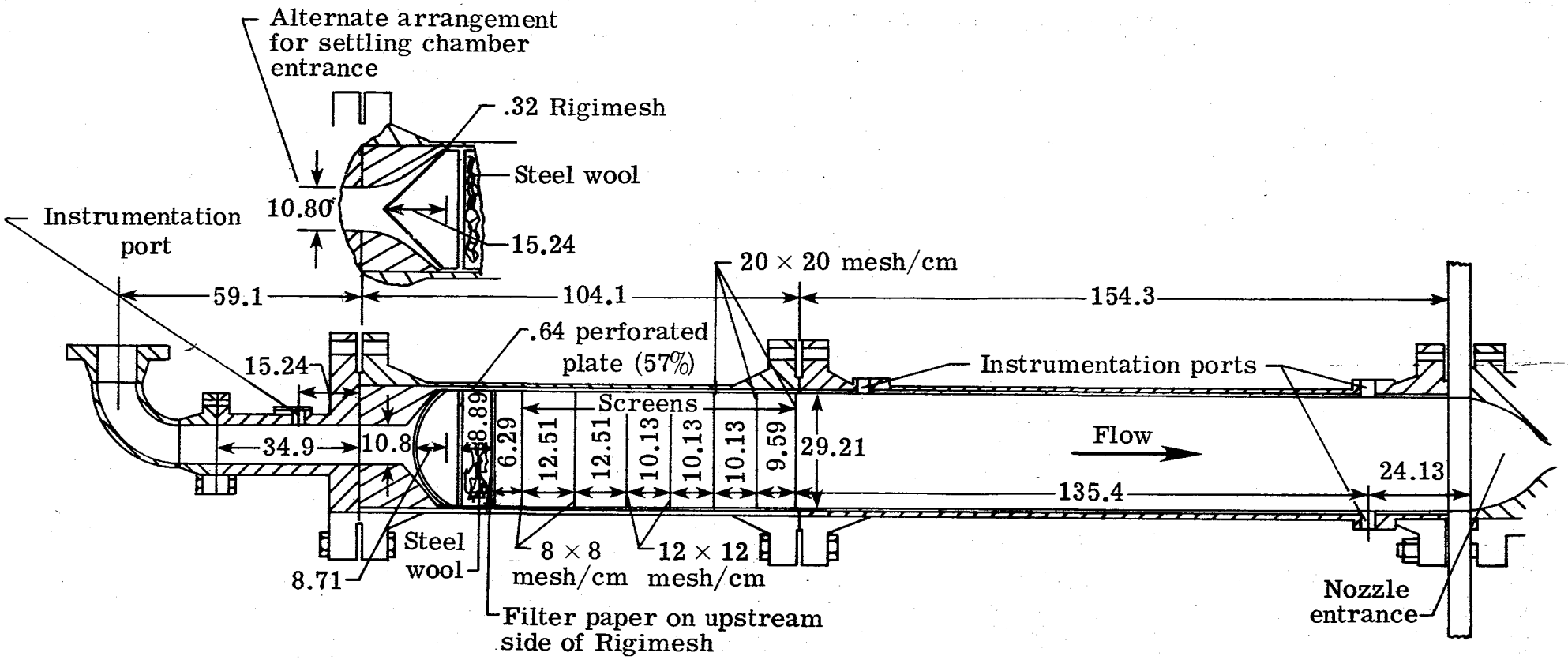

Figure 5.- Schematic scale drawing of settling chamber for the Mach 5 Quiet Tunnel from reference 18. (dimensions in cm.)

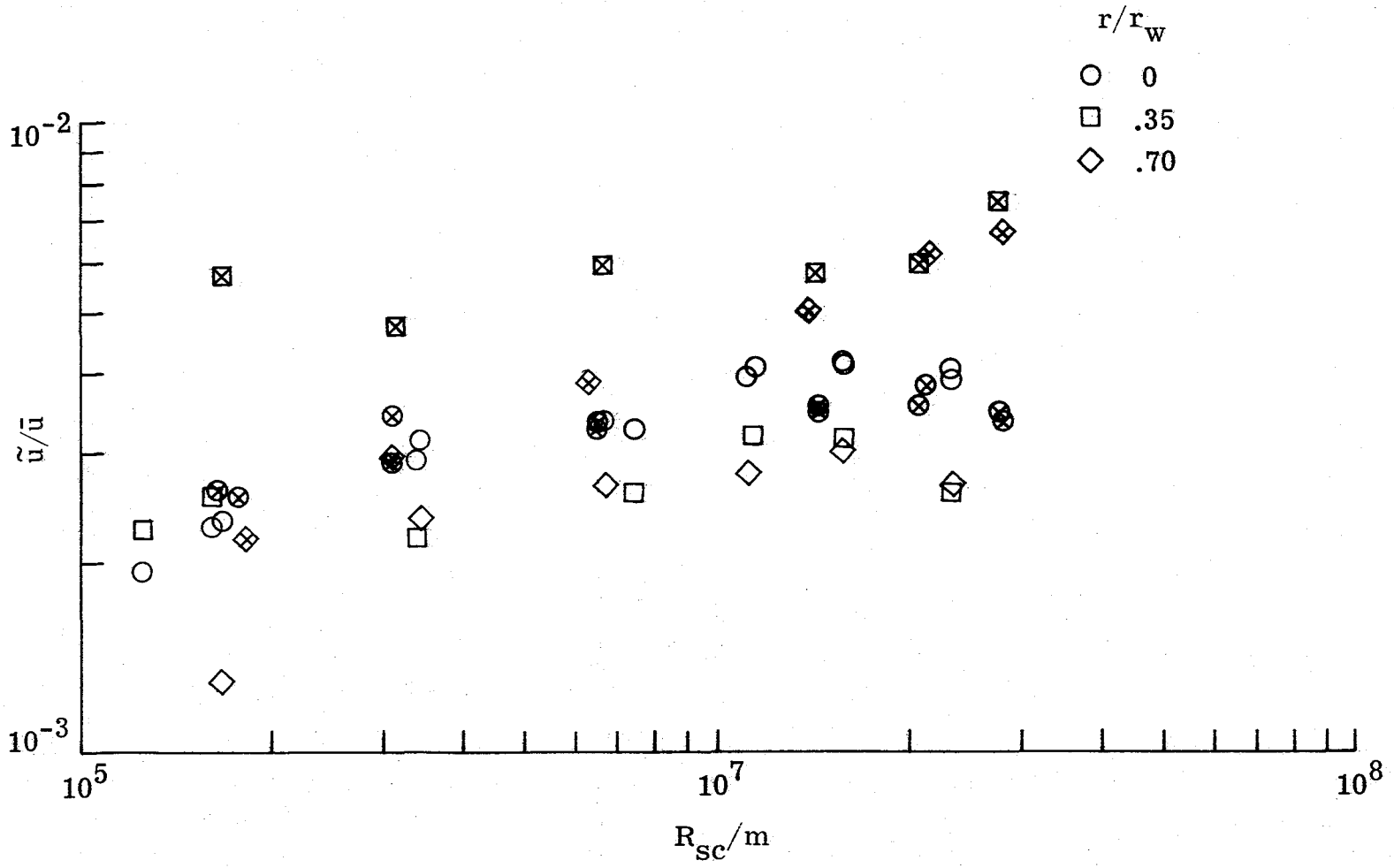

Figure 6.- Hot-wire data in settling chamber of Mach 5 Pilot Quiet Tunnel. Nozzle bleed valves open. Plain symbols are with "Rigimesh" hemisphere, × symbols are with "Rigimesh" cone. r_w = 14.61 cm (5.75 in.).

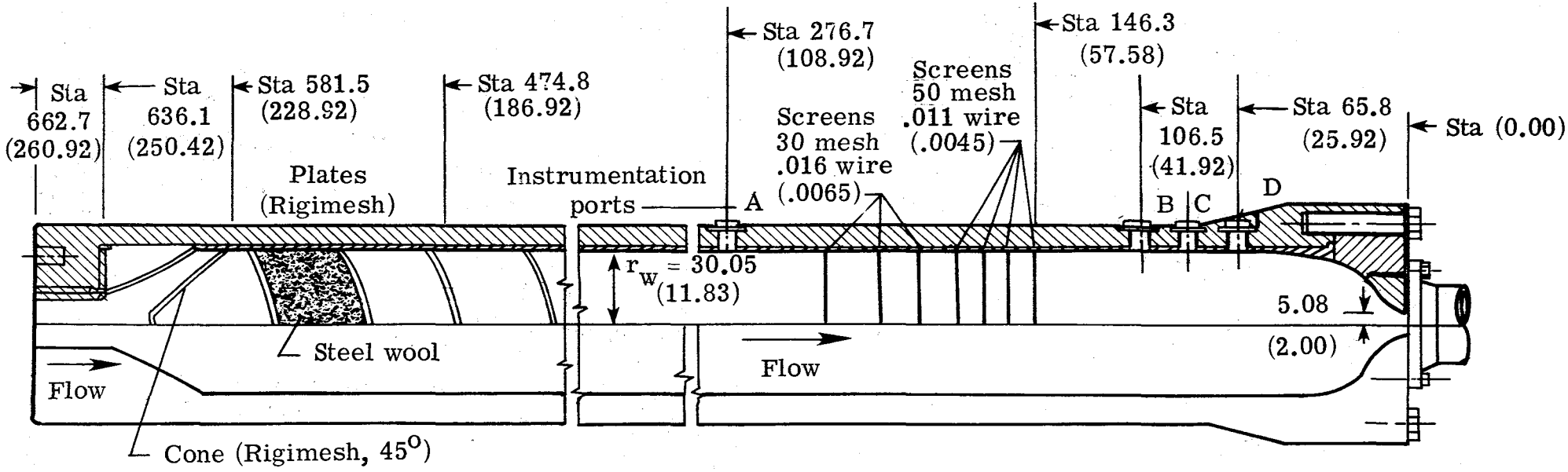

Figure 7.- Original complete settling chamber for the Supersonic Pilot Quiet Tunnel. Porous ("Rigimesh") plates and cone are 0.64 cm (0.25 in.) thick. All dimensions and stations in cm (inches).

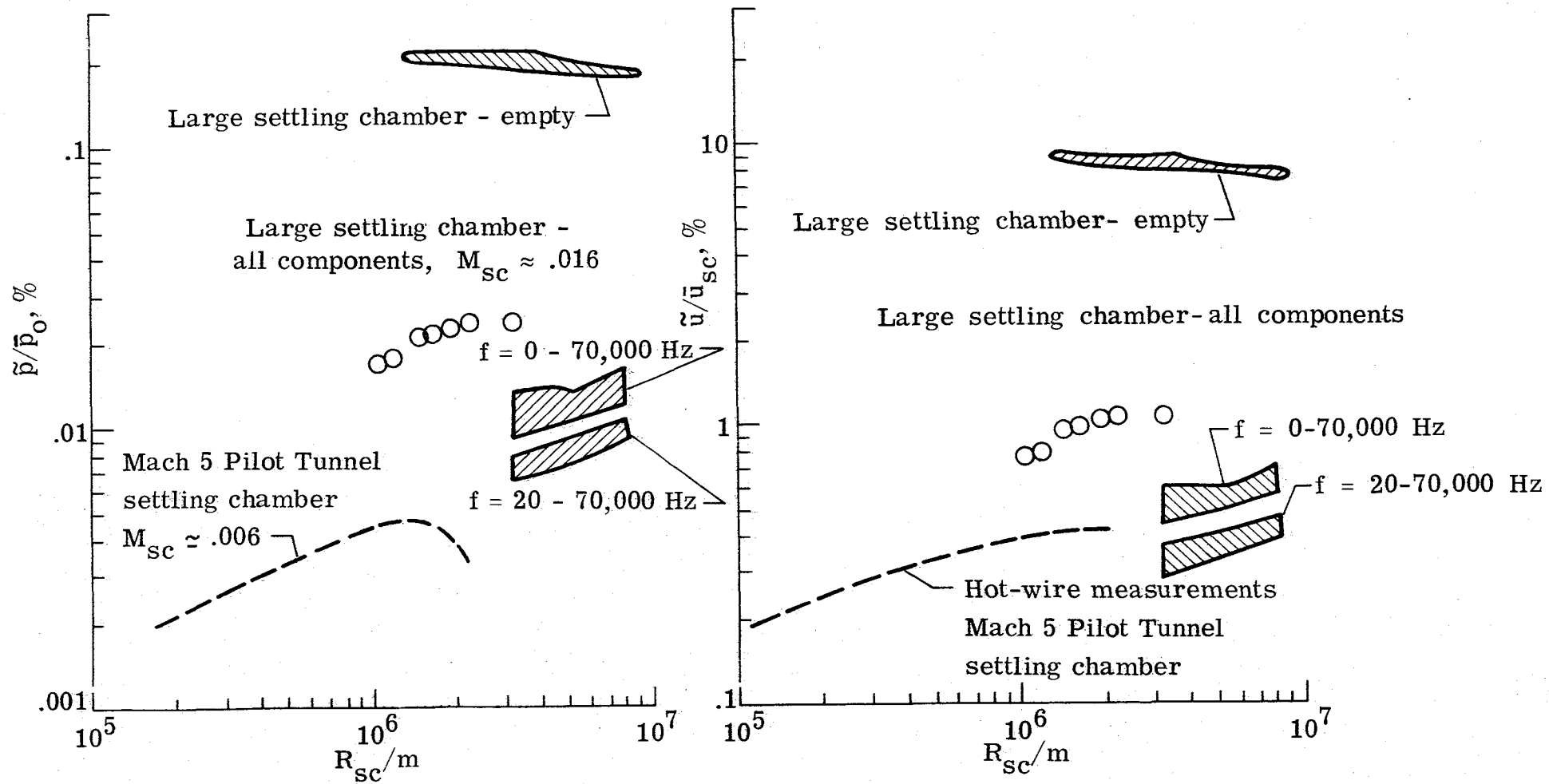

(a) Measured pressure fluctuations, except circle symbols which are hot-wire data in large chamber converted to $\tilde{p}/\bar{p}_o$ by equation (5).

(b) Velocity fluctuations from hot-wire data, except cross-hatched bands which are pressure transducer data converted to $\tilde{u}/\bar{u}_{sc}$ by equation (5).

Figure 8.- Comparison of rms pressure and velocity fluctuations in the settling chambers of the Mach 5 and the Supersonic Pilot Quiet Tunnels. All hot-wire results are on chamber centerlines only.

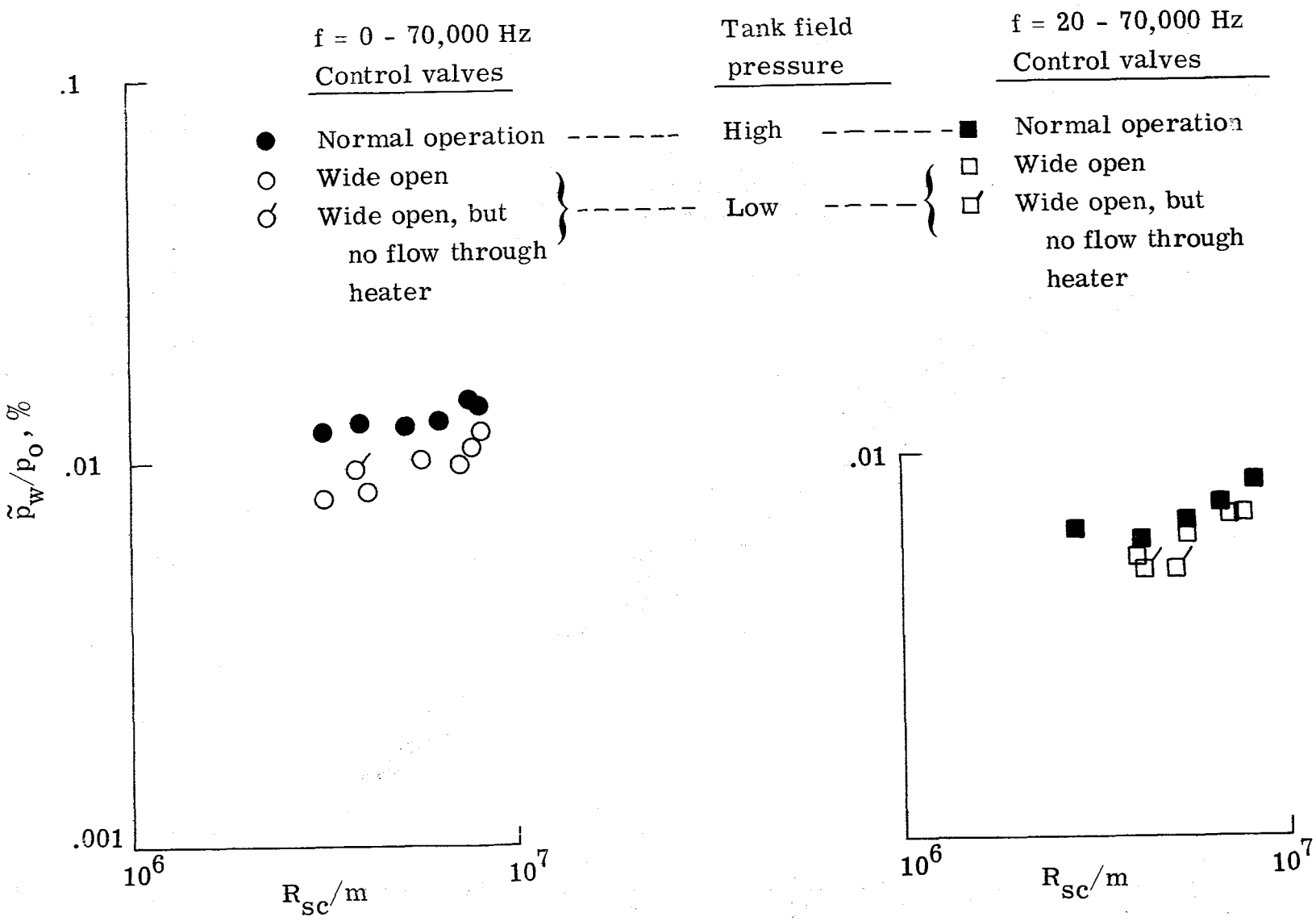

(c) Nomalized rms pressures at port D with all components installed.

Figure 8.- Concluded.

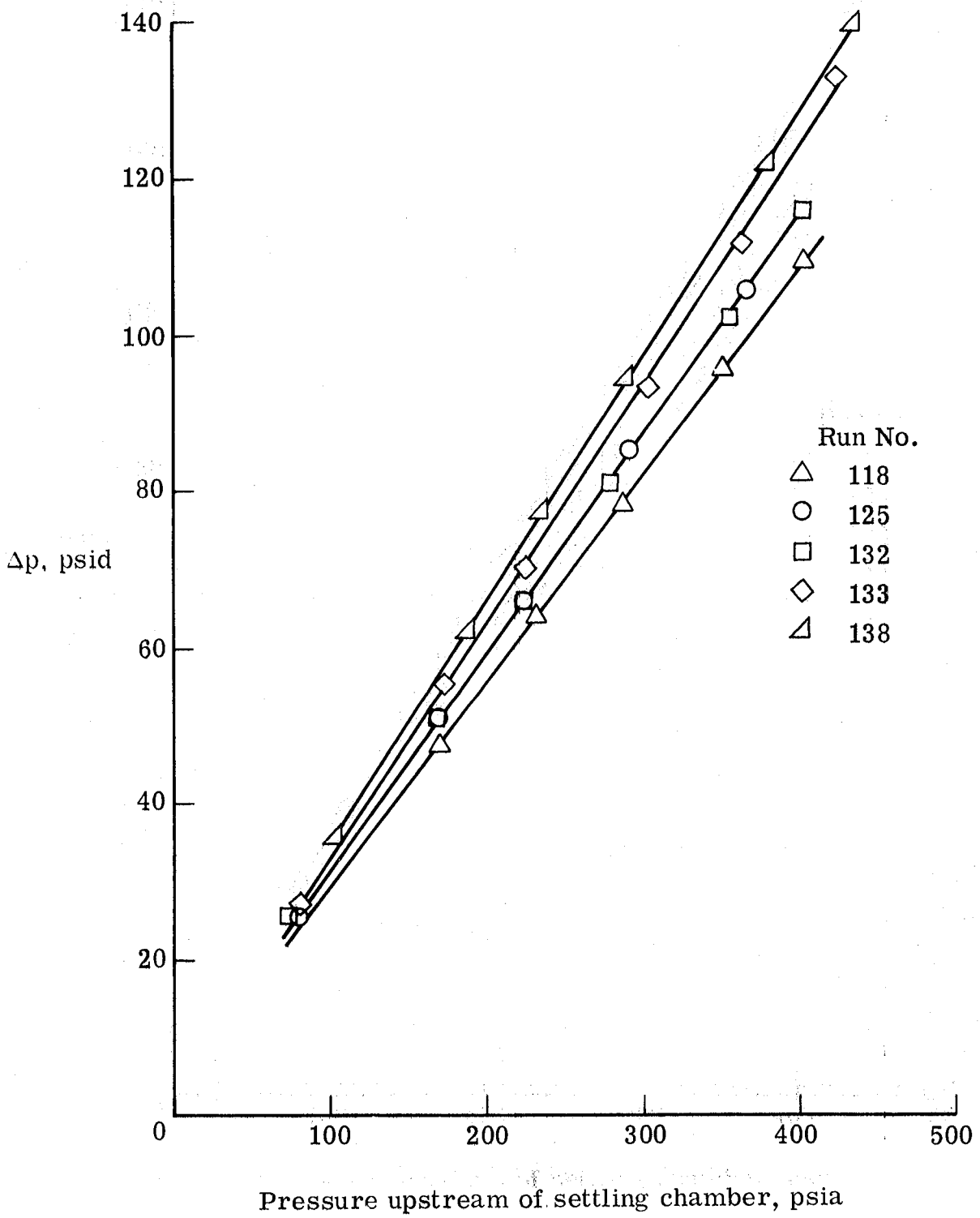

Figure 9.- Pressure drop across settling chamber of the Supersonic Pilot Quiet Tunnel with all components (fig. 7) installed.

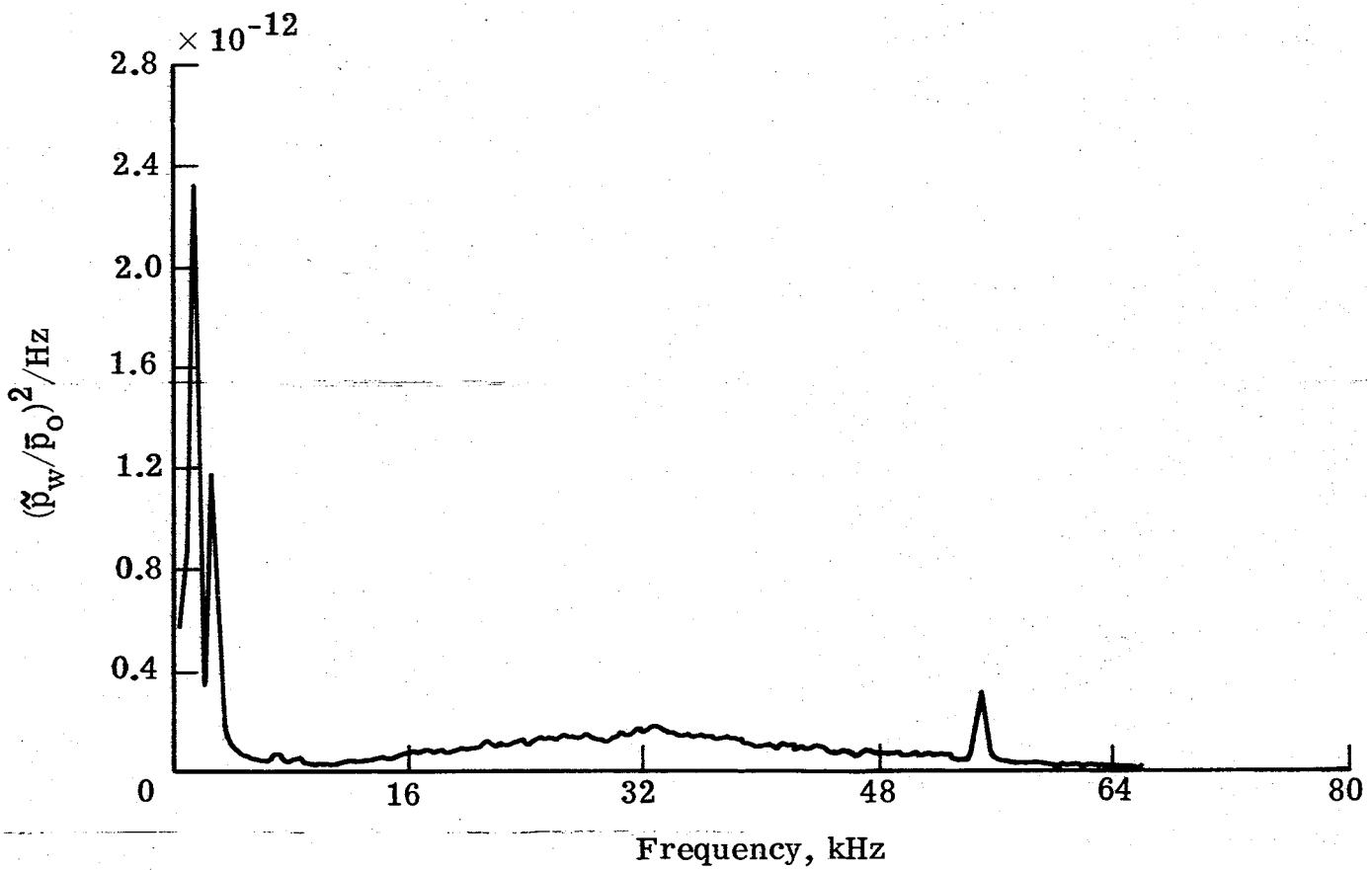

Figure 10.- Typical power spectrum from transducer mounted flush with the wall at port D. All components (fig. 7) installed. $R_{sc} \approx 6.5 \times 10^6$.

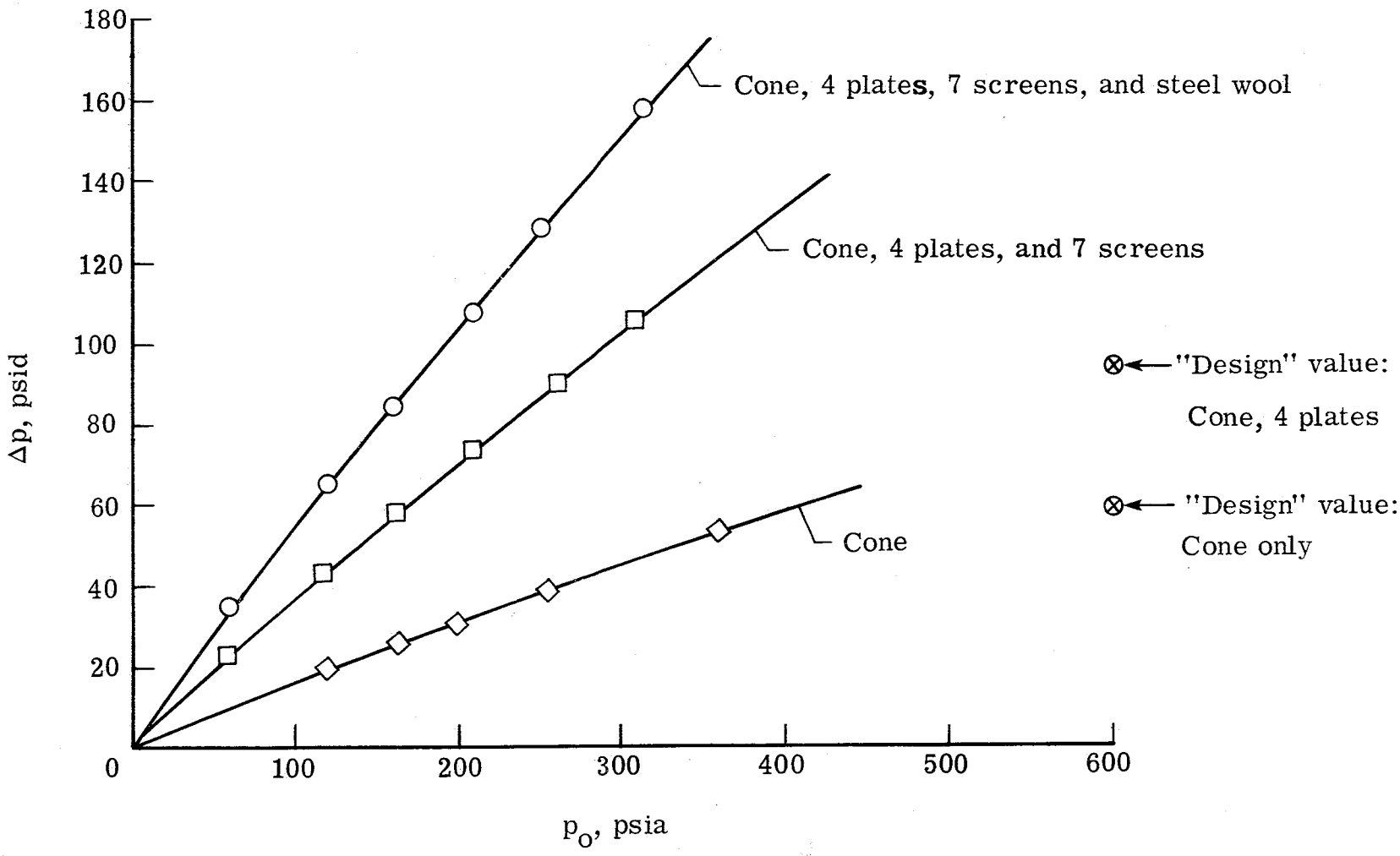

Figure 11.- Variation with stagnation pressure of the pressure drop across various components in settling chamber of the Supersonic Pilot Quiet Tunnel.
$m \approx 45$ kg/sec (100 lb/sec) at $p_o = 2400$ k Pa (350 psia).

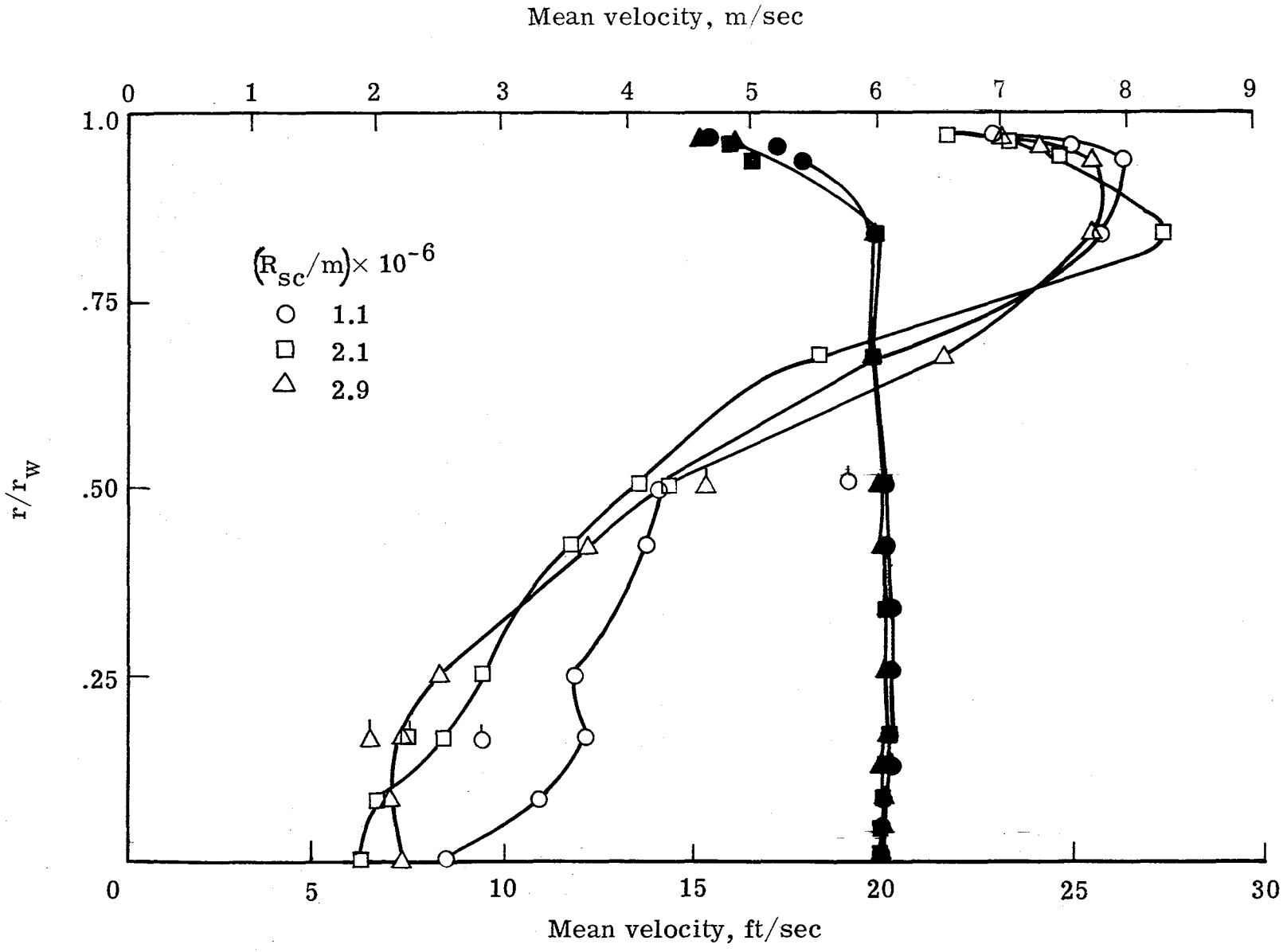

(a) Mean velocity.

Figure 12.- Velocity profiles in the complete chamber. Open symbols, Port A; closed symbols, Port B; flagged symbols, opposite side of centerline.

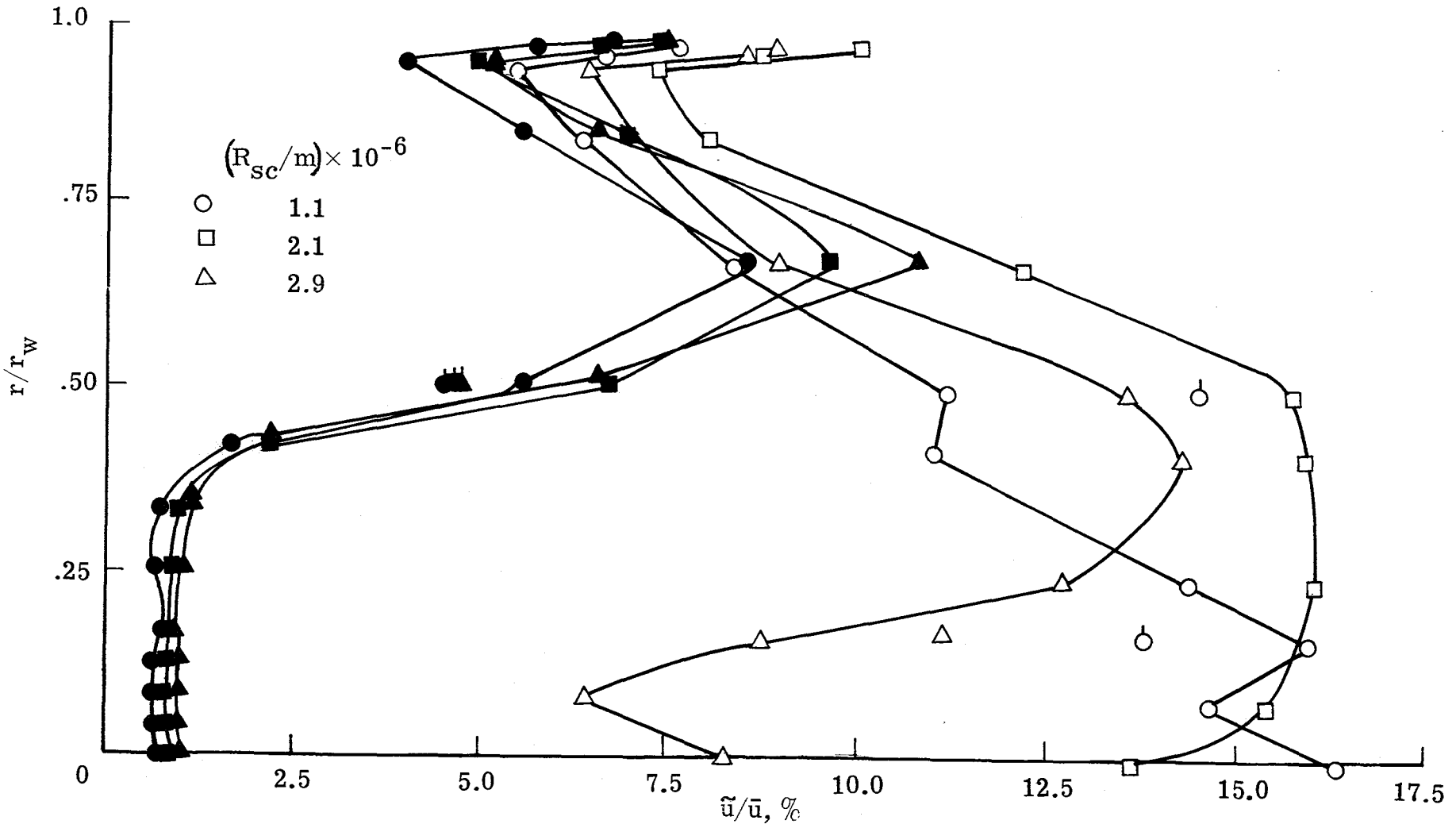

(b) rms fluctuating velocity normalized by mean velocity.

Figure 12.- Concluded.

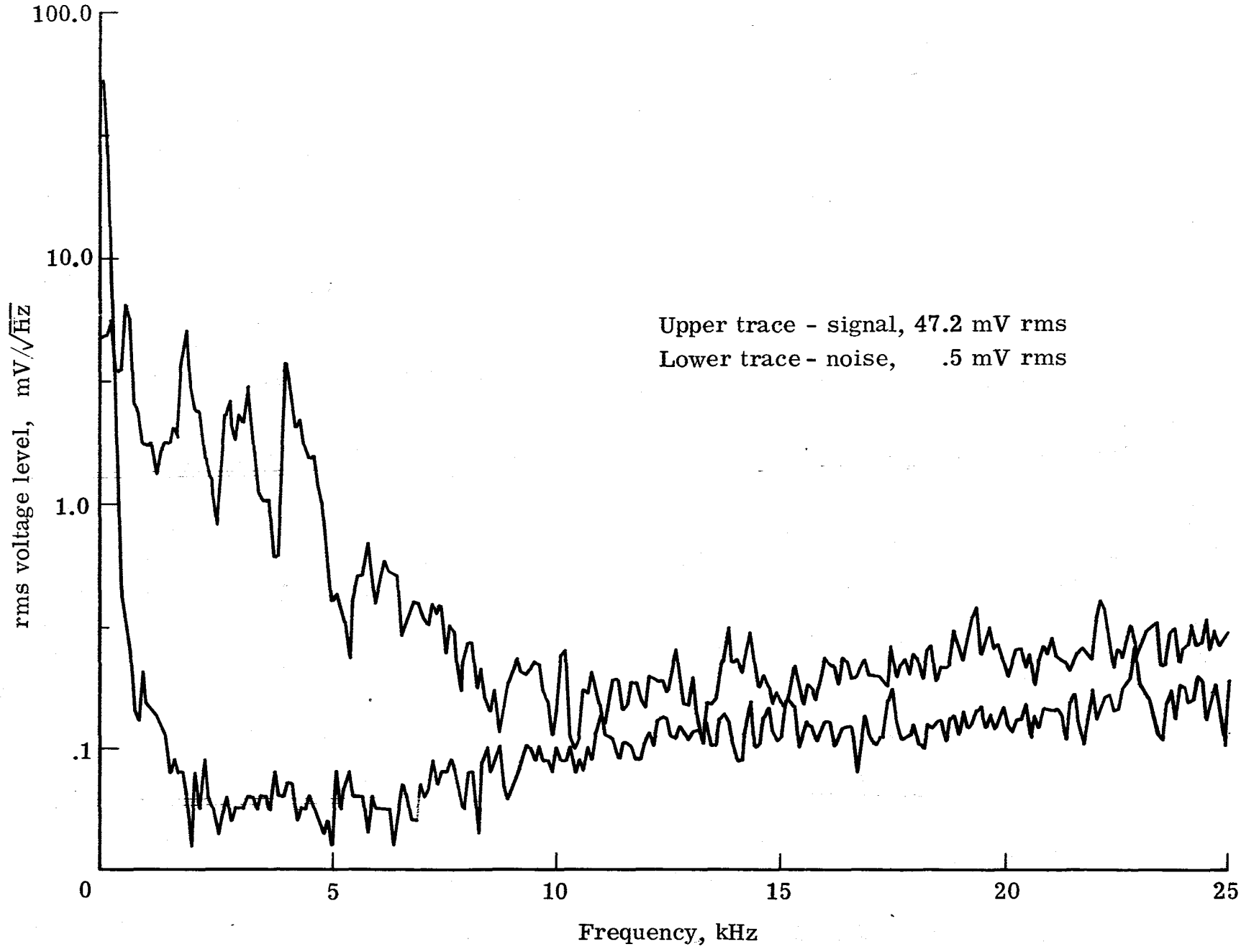

Figure 13.- Comparison of hot wire signal and electronic noise spectra at Port B.
All components installed, $r/r_w \approx 0.65$, $R_{sc}/m \approx 2.1 \times 10^6$.

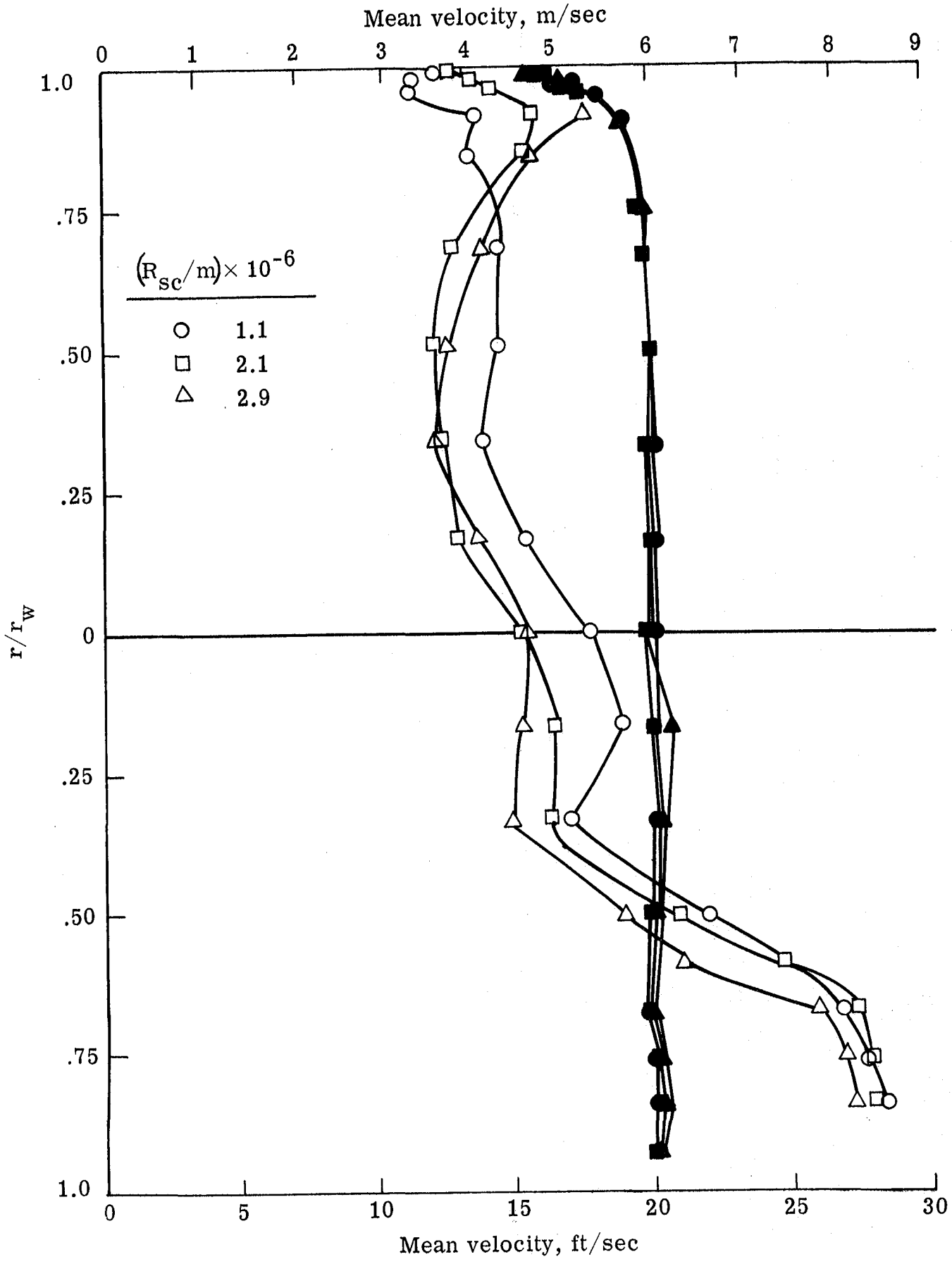

(a) Mean velocity.

Figure 14.- Velocity profiles with downstream porous plate removed. Open symbols, Port A; closed symbols, Port B.

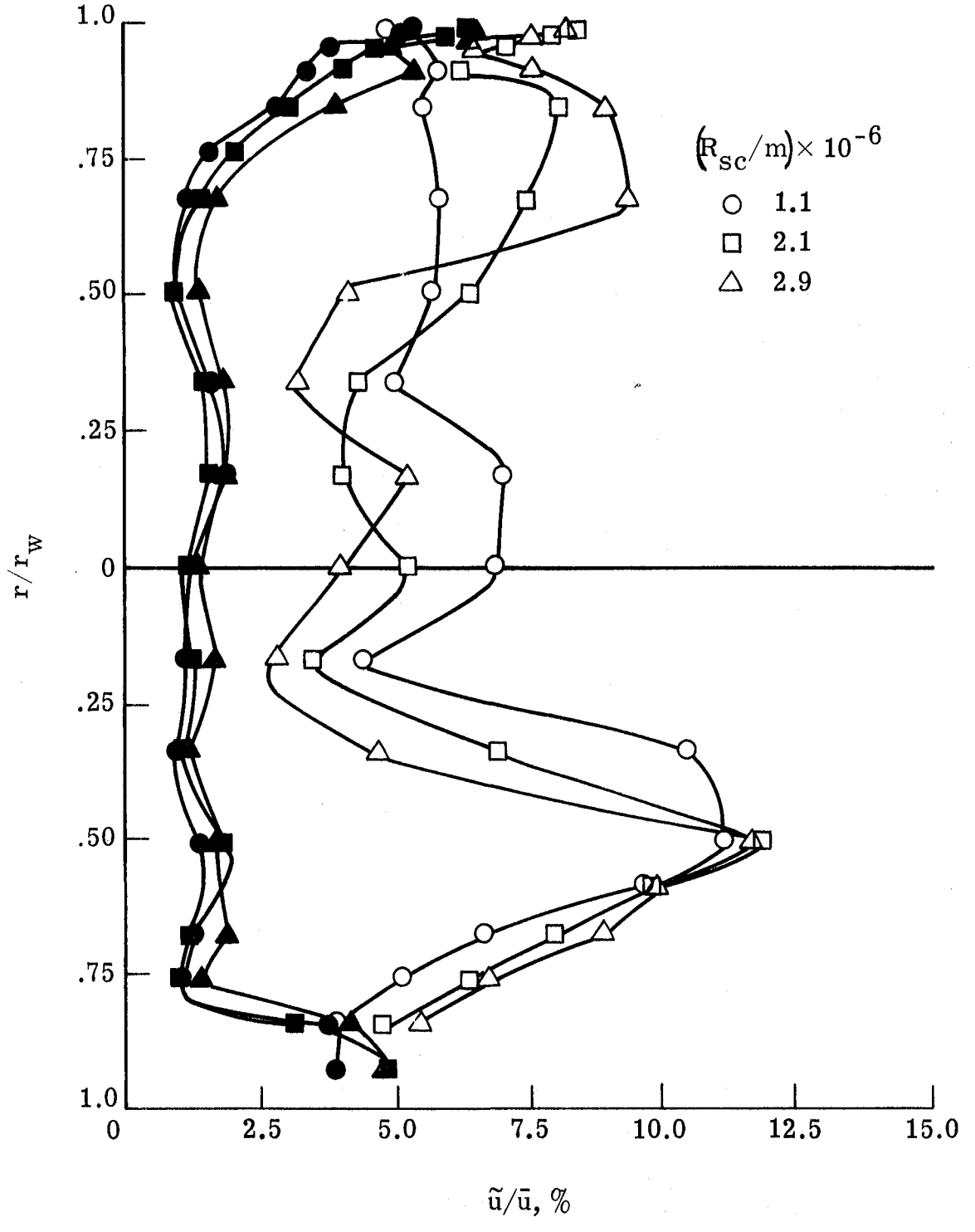

(b) rms fluctuating velocity normalized by mean velocity.

Figure 14.- Concluded.

1. Report No.	2. Government Accession No.	3. Recipient's Catalog No.
NASA TM-81948		

4. Title and Subtitle	5. Report Date
COMMENTS ON SETTLING CHAMBER DESIGN FOR QUIET, BLOWDOWN WIND TUNNELS	March 1981
	6. Performing Organization Code
7. Author(s)	8. Performing Organization Report No.
I. E. Beckwith	
	10. Work Unit No.
9. Performing Organization Name and Address	505-31-23-04
NASA Langley Research Center Hampton, VA 23665	11. Contract or Grant No.
	13. Type of Report and Period Covered
12. Sponsoring Agency Name and Address	Technical Memorandum
National Aeronautics and Space Administration Washington, DC 20546	14. Sponsoring Agency Code

15. Supplementary Notes

16. Abstract

The scheduled transfer of an existing continuous circuit supersonic wind tunnel to NASA Langley and its operation there as a blowdown tunnel has stimulated this review of flow disturbance requirements in the supply section and of recent methods developed to reduce the high level, broadband acoustic disturbances known to be present in typical blowdown tunnels. The indications are that the total turbulence levels, which include both the acoustic and vorticity modes, should be reduced to 1 percent or less in the settling chamber.

Based on recent data and the present analysis of two different blowdown facilities at Langley, methods to achieve these low levels of acoustic and vorticity disturbances are recommended. Included are pertinent design details of the damping screens and honeycomb and also the recommended minimum pressure drop across the porous components which will provide the required two orders of magnitude attenuation of the acoustic noise levels.

A suggestion for the support structure of these high pressure drop porous components is offered with the hope that detailed stress calculations and scale model tests will show whether this is a feasible approach to this most difficult problem.

17. Key Words (Suggested by Author(s))	18. Distribution Statement
wind tunnel design flow quality pipe/valve noise	Unclassified-Unlimited Subject Category 09

19. Security Classif. (of this report)	20. Security Classif. (of this page)	21. No. of Pages	22. Price*
Unclassified	Unclassified	39	A03

For sale by the National Technical Information Service, Springfield, Virginia 22161